Energy, Mines and Resources Canada

Énergie, Mines et Ressources Canada

CANMET

Canada Centre for Mineral and Energy Technology

Centre canadien de la technologie des minéraux et de l'énergie

Mining Research Laboratories

Laboratoires de recherche minière

Canada

LONG-LIVED RADIOACTIVITY ASSOCIATED WITH DUST SAMPLES FROM DENISON MINES LTD.

J. BIGU ELLIOT LAKE LABORATORY

DIVISION REPORT MRL 90-099(TR) AUGUST 1990

Work done under Denison Mines Ltd. and the Mining Research Laboratories (CANMET, E.M.R.) Research Agreement Project 143902-12-04

23pp

MICROMEDIA

91-00381/

LONG-LIVED RADIOACTIVITY ASSOCIATED WITH DUST SAMPLES FROM DENISON MINES LTD.

J. Bigu*

ABSTRACT

The α-particle activity associated with Long-Lived Radioactive Dust (LLRD) samples from an underground uranium mine has been measured. the α-particle activity measured on mine air samples has been related to the amount of silica dust collected on the samples, determined by X-ray diffraction analysis. The long-lived α-particle activity was plotted against silica dust content in the samples. A linear relationship with reasonable correlation coefficient was found which can be expressed by the equation $A = mW_Q + b$, where A and W_Q represent the α-particle activity (mBq) and silica dust mass (mg) in the sample, respectively. Because measurements of LLRD are time-consuming and expensive, the study was aimed at obtaining a useful relationship between the two variables to enable calculation of LLRD α-activity from silica dust measurements, the latter conducted on a routine basis by our laboratory for the mine under consideration. Recommendations for further studies are indicated.

Key words: Long-lived radioactive dust; Uranium mines; Underground.

*Research Scientist and Radiation/Respirable Dust/Ventilation Section Head, Elliot Lake Laboratory, CANMET, Energy, Mines and Resources Canada, Elliot Lake, Ontario.

RADIOACTIVITÉ À LONGUE PÉRIODE ASSOCIÉE AUX ÉCHANTILLONS DE POUSSIÈRES DE LA DENISON MINES LTD.

J. Bigu*

RÉSUMÉ

On a mesuré l'activité des particules α associée à des échantillons de poussières radioactives à longue période (PRLP) provenant d'une mine d'uranium souterraine. On a établi une relation entre l'activité des particules α mesurée dans des échantillons d'air de mine et la quantité de poussière de silice accumulée sur les échantillons, déterminée à l'aide de l'analyse par diffraction des rayons X. On a représenté graphiquement l'activité des particules α à longue période en fonction de la teneur en poussière de silice des échantillons. On a obtenu une relation linéaire avec un coefficient de corrélation raisonnable, qui peut être représentée par l'équation $A = mW_0 + b$, où A et W_0 représentent respectivement l'activité des particules α (mBq) et la masse de poussière de silice (mg) de l'échantillon. Comme les mesures relatives aux PRLP sont longues et coûteuses, l'étude visait à établir une relation utile entre les deux variables afin de permettre le calcul de l'activité α des PRLP à partir de mesures portant sur la poussière de silice, ces dernières étant effectuées de façon périodique par notre laboratoire pour la mine considérée. Des recommandations concernant d'autres études sont présentées.

Mots-clés : poussière radioactive à longue période; mines d'uranium; mine souterraine.

*Chercheur scientifique et chef de la section Rayonnement/poussière inhalable/ventilation du Laboratoire d'Elliot Lake, CANMET, Énergie, Mines et Ressources Canada, Elliot Lake (Ontario).

CONTENTS

	Page
ABSTRACT	i
RESUME	ii
INTRODUCTION	1
THEORETICAL BACKGROUND	2
EXPERIMENTAL PROCEDURE	4
EXPERIMENTAL RESULTS AND DISCUSSION	5
FURTHER COMMENTS	10
CONCLUSIONS	11
ACKNOWLEDGEMENTS	13
REFERENCES	13

TABLES

1. LLRD, respirable dust (RD) and silica dust (S_iO_2) data from Denison Mines Ltd	15

FIGURES

1. Scaler background (α-particle) count rate frequency histogram	26
2. Scaler background (α-particle) count rate frequency histogram	27
3. Scaler background (α-particle) count rate frequency histogram	28
4. Scaler background (α-particle) count rate frequency histogram	29
5. Scaler background (α-particle) count rate frequency histogram	30
6. Scaler background (α-particle) count rate frequency histogram	31
7. Quartz dust mass frequency histogram	32
8. Quartz dust mass frequency histogram	33
9. Silica (quartz) dust concentration frequency histogram	34
10. LLRD α-particle activity frequency histogram	35
11. LLRD α-particle activity frequency histogram	36
12. LLRD (α-particle) activity frequency histogram	37
13. Specific activity (ratio of LLRD α-particle activitry and quartz dust mass) frequency histogram	38
14. $[S_iO_2]$ - $\overline{[S_iO_2]}$ frequency histogram	39
15. $[S_iO_2]$ - $\overline{[S_iO_2]}$ frequency histogram	40
16. [LLRD] - $\overline{[LLRD]}$ frequency histogram	41
17. [LLRD] - $\overline{[LLRD]}$ frequency histogram	42

18. LLRD α-particle activity versus respirable dust mass 43
19. LLRD α-particle activity versus respirable dust mass 44
20. LLRD α-particle activity versus respirable dust mass 45
21. LLRD α-particle activity versus quartz dust mass for underground miners 46
22. LLRD α-particle activity versus quartz dust mass for mill workers ... 47
23. LLRD α-particle activity versus quartz dust mass for 'other' workers. 48

INTRODUCTION

In underground uranium mines and uranium mills, dust emissions contain many radionuclides. These radionuclides have been identified by a variety of methods, such as α- and γ-spectroscopy, neutron activation analysis, particle induced X-ray emission, fluorescence, and spectrophotometry (1-4). The radionuclides identified include the parents of the natural uranium and thorium decay chains (^{235}U, ^{238}U, and ^{232}Th), and their short-lived and long-lived decay products. Dust that contains long-lived radionuclides is commonly referred to as Long-Lived Radioactive Dust (LLRD).

The inhalation of dust generated in mining and milling operations poses a potential health hazard, and if the dust contains long-lived radionuclides, inhalation can pose a far greater occupational health hazard. Because of the health risks associated with the inhalation of LLRD, its accurate characterization and quantification is of great practical importance in order to calculate personal occupational exposures.

Because radionuclides are contained in uranium (U) ores, and hence in dust particles produced in the course of unit mining and milling operations, the hypothesis has been suggested that there might be a relationship between dust collected on filters and the radioactivity associated with the dust (5). This suggestion has been partly confirmed when radioactivity (α-particle) measurements were carried out on a number of air samples (taken from underground uranium mines and uranium mills) on which total dust and silica dust mass measurements had previously been made as part of a routine program conducted by the Elliot Lake Laboratory for a uranium mining company. The air samples measured and analyzed in this study corresponded to samples collected during the period 1987-1990. The present investigation was requested by Denison Mines Ltd.

THEORETICAL BACKGROUND

The uranium deposits corresponding to the mine where dust samples were taken consist of layers and channels of Precambrian, pyrite-rich, quartz-pebble conglomerate. The minerals within the conglomerates mainly consist of pyrite, brannerite (uranium titanate) and uraninite (uranium oxide) which are associated with varying amounts of uranothorianite (silicate of uranium and thorium), among other minerals. The U and Th minerals are associated mainly with sulphides, e.g., pyrites. The minerals occur interstitially to the quartz pebbles in the conglomerate matrix.

A quantitative study on the relationship between dust and the radioactivity associated with it is by no means trivial or straightforward. In such studies the following should be given careful consideration:

1. α-particle self-absorption effects, i.e., α-particle energy degradation and α-particle absorption in the dust layer deposited on the filter during air sampling;
2. Characteristics of the dust deposited on the filter, e.g., chemical composition, size distribution, and electrical charge; and
3. Type of dust sampling device, e.g., particle size threshold, cut-off size and other parameters.

Item 1 depends, in turn, on the following:

a) α-particle energy, i.e., radioisotope under consideration;
b) spatial distribution of dust deposition on the filter;
c) thickness of the dust layer;
d) dust size distribution;
e) chemical composition of the dust, i.e., atomic number of the different constituents if more than one.

Item 2 is a function of the following items:

a) mining and milling operations such as crushing, blasting, drilling, slushing, mucking, transportation, leaching, etc.;

b) mining and milling activities such as vehicle traffic, personnel traffic, wetting, etc.;

c) environmental factors such as relative humidity and temperature; and

d) airflow conditions, recirculation paths, air leakages, etc. at the working location.

In the investigation reported here, however, some of the above items have not been considered in detail for lack of pertinent information and/or for the sake of simplicity. For example, data (i.e., samples) were collected using only one type of sampling device (nylon cyclone) and always following the same operational procedure. Furthermore:

a) no direct size distribution data are available because no concurrent measurements of size distribution, with say multistage cascade impactors or particle size optical counters, were conducted; and

b) because of an insufficient number of samples for statistical confidence, no attempt has been made to separate samples according to different mining operations. Hence, all mining operations have been lumped together for the purpose of statistical analysis. However, because not all the samples were taken underground but also at the mill, as well as other mine locations, the samples have been separated and analyzed according to three main groups, namely, underground miners, mill workers, and other personnel. Finally, the three groups were analyzed together.

The data presented here have been obtained in the analysis of about 1,000 samples taken during the period 1987-1990. One important consideration of which the reader should be aware is that because of the long half-life of the radioisotopes measured, the α-particle activity associated with the dust samples is rather low. Hence, the statistical error associated with the radioactivity measurements is in some cases quite significant.

EXPERIMENTAL PROCEDURE

Dust samples were taken at an underground uranium mine at a variety of mine working locations. Dust samples were collected on silver membrane filters (5 μm mean pore size) using dust samplers of the nylon cyclone type. Total dust mass and quartz dust mass in the respirable range (<1-10 μm) were estimated. Total dust mass was measured by weighing the filters before and after the samples were collected. Quartz dust was measured by X-ray diffraction analysis (6).

Alpha-particle activity from long-lived radionuclides associated with dust samples was estimated by gross α-count using α-particle counters with a ZnS(Ag) screen optically coupled to a photomultiplier tube, and associated electronic circuitry, as the α-particle detector. Alpha-particle measurements were made no earlier than one month after the dust samples were taken. This procedure was followed to ensure, quite conservatively, complete decay of airborne short-lived decay products of radon (^{222}Rn), and thoron (^{220}Rn) collected in the filter during sampling. It should be noted that the short-lived decay products of ^{222}Rn and ^{220}Rn arise from the decay of a) long-lived radionuclides, such as ^{226}Ra, in dust; and b) ^{222}Rn and ^{220}Rn in mine air. The short-lived radioactivity from item b) is referred to as airborne activity and, although collected during sampling, is not associated with dust, i.e., item a). Radioisotope identification was carried out by α-spectrometry as discussed elsewhere (1,3,4).

Gross α-particle activity in each sample was measured as follows. Three 30 min α-particle background count measurements were taken daily for each counting instrument, i.e., scalers. Six scalers were used, which enabled six samples to be measured simultaneously. Each sample was counted twice sequentially for 45 min each time. The average values for the background and sample α-count, in counts per second (cps), were calculated. The difference in α-count, i.e., net α-count, was computed. The net α-count was converted

into absolute disintegration rate, in disintegrations per second (dps), i.e., Becquerels (Bq), where, by definition, 1 Bq = 1 dps.

The airborne α-particle activity concentration, A_s, in Bq/m^3, is given by Equation 1:

$$A_s = 10^3 \, A/QT_s \qquad \text{Eq 1}$$

where, Q is the air sampling flow rate in L/min, and T_s is the sampling time in min. The symbol A is the long-lived α-particle activity measured in Bq in the dust sample. This activity is given by $A = \hat{N}_\alpha/\epsilon$, where $\hat{N}_\alpha$ is the average net α-particle count in cps, and ϵ is the α-particle counting efficiency of the α-particle counter used. The efficiency of the counter was determined using a standard ^{241}Am source of activity traceable to the U.S. National Bureau of Standards.

Alpha-particle counting was conducted using detector/counter arrangements (scalers for brevity) consisting of a 25 mm diameter ZnS(Ag) screen optically coupled to a photomultiplier tube and associated electronic circuitry, model Tri-Met 372A, manufactured by Tri-Met Instruments, Winnipeg, Canada.

In contrast to other previous LLRD studies, no dust mass selection was done this time, i.e., all the available samples were counted for α-particle activity regardless of how low their dust mass was (5-7). The samples analyzed here are representative of a variety of mining and also milling operations. Because no concurrent dust size distribution measurements were conducted, important parameters such as the Mass Median Aerodynamic Diameter (MMAD) and the Activity Median Aerodynamic Diameter (AMAD) are not known. Analysis of the samples was mainly done by linear regression techniques using the least squares method.

EXPERIMENTAL RESULTS AND DISCUSSION

The analysis of the data obtained has been summarized in Figures 1 to

23 and Table 1.

Figures 1 to 6 show frequency histograms of background readings from the six scalers used in the measurement of α-particle activity from LLRD samples. The Figures show that except from one scaler (see Figure 2, scaler No. 5), above 80% of the background α-particle count rate measurements were less than about 0.25 cpm (counts per minute). For scaler No. 5, the count rate in over 80% of the cases was about 0.4 cpm. These background values indicate that the α-particle background activity of the scalers used was quite adequate for low activity measurements of LLRD, and hence, they give a high degree of confidence in the reliability of the experimental data derived from LLRD sample measurements.

Figures 7 to 9 show frequency histograms of the quartz dust mass accumulated in the Ag membrane filters used during the sampling period (Figures 7 and 8) and of the airborne quartz dust mass concentration (Figure 9), both obtained by X-ray diffraction analysis of the LLRD samples. A best fit from the data was obtained by linear regression analysis (Figure 8). The result of this analysis can be represented by the following expression:

$$f = 195.11\, e^{-37.145(S_iO_2)} \qquad \text{Eq 2}$$

where, f (frequency) represents the number of samples of quartz dust mass content denoted by (S_iO_2).

Figure 9 shows that a majority (~90%) of the samples collected represented airborne quartz dust concentration below ~0.1 mgm^{-3}.

Figures 10 to 12 show frequency histograms of the α-particle activity corresponding to the LLRD accumulated on the filters during the sampling period (Figures 10 and 11), and of the airborne LLRD concentration, [LLRD], see Figure 12. The α-particle activity measured on the samples was below ~15 mBq in a majority of the cases (>80%). Figure 10 can be represented by the analytical expression (see Figure 11):

$$f = 84.77\, e^{-0.1604(LLRD)} \qquad \text{Eq 3}$$

where, f represents the number of samples of LLRD α-particle activity denoted by (LLRD).

Figure 12 shows that in over 80% of the cases the airborne LLRD concentration, denoted [LLRD], was less than about 25 $mBqm^{-3}$, with ~70% falling below 10 $mBqm^{-3}$. This indicates that more often than not the [LLRD] was lower rather than higher.

Figure 13 shows a frequency histogram of the airborne quartz dust specific activity, i.e., the α-particle activity per unit mass of quartz dust. About 80% of the samples had a specific activity $\lesssim 600$ $mBqmg^{-1}$. However, a wide spread in specific activity (SA) has been measured, namely, $\gtrsim 2 \times 10^3$ $mBqmg^{-1}$ (only ~10% of the samples had SA $\gtrsim 1.0 \times 10^3$ $mBqmg^{-1}$). This histogram suggests the following. One would expect that for a given LLRD size distribution, mining operation, constant or fixed ore grade, and assuming isotropy and homogeneity of mineral composition, and that no α-particle absorption effects in silica (quartz) dust take place, the SA frequency distribution should be single-valued or nearly single-valued. The fact that a broad range of values for the Long-Lived Radioactive Dust (LLRD) Specific Activity (SA) is obtained is clearly indicative that different size distributions, most likely arising from different mining operations, inhomogeneity of sample composition, and self-absorption effects, are operative. The results are very important and under investigation.

Figures 14 and 15 show frequency histograms of the difference $[S_iO_2] - \overline{[S_iO_2]}$, where, $[S_iO_2]$ stands for the airborne quartz $[S_iO_2]$ dust mass concentration, and $\overline{[S_iO_2]}$ indicates the arithmetic mean of the same variable calculated taking all the available samples. The only difference between Figures 14 and 15 is the range of values for the variable $[S_iO_2] - \overline{[S_iO_2]}$ which is 10 times larger (i.e., up to 2 mgm^{-3}) for the former (Figure 14) than for the latter, i.e., up to 0.2 mgm^{-3} (Figure 15). These Figures indicate a strong bias towards samples having airborne quartz dust mass concentration

significantly lower than the arithmetic mean of the entire population of samples measured.

Figures 16 and 17 show frequency histograms of the difference [LLRD] - $\overline{[LLRD]}$ where, [LLRD] is, as usual, the airborne LLRD concentration measured on the sample (α-particle activity), and $\overline{[LLRD]}$ represents the arithmetic mean of the same variable calculated taking all the available samples. The only difference between Figures 16 and 17 is in the range of values chosen for the quantity [LLRD] - $\overline{[LLRD]}$ which is substantially lower (i.e., up to 30 $mBqm^{-3}$) for Figure 16 than for Figure 17, i.e., up to 560 $mBqm^{-3}$. Similarly, as in the case of $[S_iO_2]$ - $\overline{[S_iO_2]}$, Figures 16 and 17 show a strong bias in favour of samples having lower airborne [LLRD] than the arithmetic mean of the whole sample population measured.

Figures 18 to 23 show α-particle activity from LLRD samples, i.e., (LLRD), versus respirable dust mass, (RD), (Figures 18 and 19) and α-particle activity from LLRD samples versus quartz dust mass, (S_iO_2), (Figures 20 to 23). Also shown in these Figures are the best fitted lines by regression analysis using the Least Squares method. Figures 21 to 23 show data for three distinct mine personnel 'groups', whereas Figure 20 shows the same kind of data but for all groups together, i.e., combined. It should be noted that although, as previously indicated, the number of samples analyzed was approximately 1,000, a number of these samples has not been included in the final analysis for a variety of reasons, the most important being the very low α-particle activity associated with them (lower than the average scalers' background) which gave negative values for the net α-particle count rates. Hence, the total number of samples included in the final analyses has been reduced from the original 1,000 to slightly higher than 600!

The correlation expressions corresponding to Figures 18 and 19 are, respectively:

$$(LLRD) = 34.618\ (\pm 2.0)\ (RD) + 1.21\ (\pm 18.4), \quad \text{and} \qquad \text{Eq 4}$$

$$(LLRD) = 6.409\ (\pm 17.1) + 3.195\ (\pm 3.64)\ (RD) + 13.947\ (\pm 1.39)\ (RD)^2 \qquad \text{Eq 5}$$

where, (RD) represents the respirable dust mass of the sample which includes silica dust, other mineral dusts and diesel particulates.

Equation 4 corresponds to a straight line, whereas Equation 5 corresponds to a second order polynomial expansion. These two expressions have been obtained for the same sample population. The low correlation coefficients obtained in both cases indicate that their use would be very limited to obtain information of (LLRD), in mBq, from (RD), in mg.

Regression analysis of the data in Figure 20 (606 samples) shows that the relationship between (LLRD) and quartz dust mass (S_iO_2) can be expressed as follows:

$$(LLRD) = 145.24\ (\pm 3.8)\ (S_iO_2) + 3.26\ (\pm 12.2) \qquad \text{Eq 6}$$

Finally, the samples were analyzed according to three main personnel groups, namely, underground miners (Figure 21), mill workers (Figure 22), and 'other personnel' (Figure 23). Regression analysis in these three cases show that the Long-Lived Radioactive Dust α-particle activity on the sample, i.e., (LLRD) can be expressed as a function of the silica (quartz) dust mass on the same sample, i.e., (S_iO_2), by the following expressions:

1. UNDERGROUND MINERS

$$(LLRD) = 141.94\ (\pm 7.89)\ (S_iO_2) + 1.34\ (\pm 6.55) \qquad \text{Eq 7}$$

The total number of samples analyzed was 241, and the correlation coefficient, R, corresponding to the above expression was: R ~0.8.

2. MILL WORKERS

$$(LLRD) = 225.94\ (\pm 13.35)\ (S_iO_2) + 14.03\ (\pm 22.33) \qquad \text{Eq 8}$$

The total number of samples used was 54, and the correlation coefficient for Figure 22 was: R ~0.92.

3. OTHER WORKERS

In this case, the expression obtained was:

$$(LLRD) = 164.84\ (\pm 5.89)\ (S_iO_2) + 4.08\ (\pm 7.84) \qquad \text{Eq 9}$$

The number of samples examined in this case was 123, and the correlation coefficient obtained was, R ~0.93.

Expressions 5), 7) and 9) do not differ by more than about 10% from previous expressions reported elsewhere (5). For mill workers, Equation 8 shows that although a higher slope was obtained than that reported in the expressions of reference 5, as well as other expressions in this report, this slope is still within the range of values obtained in other analyses of samples taken at several underground uranium mines in the Elliot Lake area.

Although the present study was also aimed at analyzing the relationship between LLRD and S_iO_2 for a variety of mining operations and miner occupations, the lack of pertinent data, but above all, the scarcity of samples for confident statistical analysis have precluded further analysis of these samples except for the three main 'personnel' groups referred to above (see Equations 7 to 9).

FURTHER COMMENTS

The analysis of the data presented in this report suffers from two major weaknesses, namely:

1. α-particle self-absorption effects have not been taken into account;
2. No dust size characterization data are available;
3. No adequate number of samples is available for an analysis according to mining operations and miner's occupation.

Because different mining operations are generally characterized by significant differences in radioactivity (and dust mass) versus dust size distribution, analysis of samples according to mining operations is of vital importance. Furthermore, the AMAD and MMAD of the LLRD α-particle activity and particle size distributions, respectively, may influence α-particle self-absorption substantially. Unfortunately, data on mining operations and LLRD characterization were not available to be included in the present analysis.

It is clear from the above that LLRD characterization (i.e., α-particle activity and particle size distribution) is of paramount importance in order to interpret field data. However, the actual airborne LLRD characterization is not the only item of practical interest, but more importantly, the particle size sampling characteristics of the sampling device, such as cut-off size, etc., play a major role. This is so because different dust sampling devices sampling the same dust atmosphere collect significantly different size distributions or size fractions on the collecting filter.

Finally, with regard to α-particle self-absorption, the following considerations are important in the calculation of self-absorption effects:

1. Spatial distribution of LLRD in the filter. The spatial distribution depends on the sampling device used, e.g., size cut-off, sampling 'head' geometry, sampling flowrate, and other parameters. The LLRD spatial distribution can be studied using scanning techniques such as electron microscopy.
2. Thickness of LLRD on the filter. This parameter is difficult to estimate because of item 1. An average value for the LLRD layer thickness can be calculated from the total LLRD mass and the surface area covered by it.

CONCLUSIONS

The main conclusions that can be derived from this study are the following:

1. No 'good' correlation between LLRD and total respirable dust could be found.
2. Correlations between LLRD and quartz dust were obtained with relatively high correlation coefficients, i.e., $0.8 \leq R \lesssim 0.92$.
3. The relationships found between LLRD and quartz (silica) dust mass were within ~10% of the values previously reported elsewhere, except for data obtained for the mill workers which were, neverthereless, within the range

of values calculated in other independent studies.

4. The relationships obtained in items 1 and 2 are not site-specific or mining operation specific. They are rather of a general nature obtained by lumping together all the available data.
5. The data reported here have a weakness because they are not related to item 4, and because of lack of information regarding dust size and radioactivity characterization (e.g., MMAD and AMAD), and chemical make-up and ore grade.

Hence, in order to be able to draw confident and accurate conclusions regarding the meaning of the data obtained in this and other similar studies, the following items are recommended:

A. New data should be collected according to mining operation and miner's occupation.
B. Item A should also be accompanied by data regarding dust radioactivity and size characterization as well as information on ore grades, ventilation conditions and other environmental data.
C. Adoption of a given instrument so that data obtained with this instrument (i.e., sampling device) can be readily compared.
D. Thorough study of the sampling characteristics of the sampling device chosen, or rather adoption of the most suitable instrument available, compatible with physical, practical and economic constraints.
E. Careful study of the errors associated with the measurement of LLRD α-particle activity with regard to self-absorption and other effects.

In spite of the obvious limitations of the data presented here, the expressions obtained are useful and of practical value when no great accuracy is required. The reader should be aware that no 'better' data will be obtained by simply taking more samples unless the above items, i.e., requirements, are met. However the extra effort may not result in any dramatic improvement in the quality of these data. Also it is very doubtful

that a correlation coefficient greater than 0.9 can consistently be attained in view of the great practical and experimental difficulties encountered in projects of this nature.

ACKNOWLEDGEMENTS

The author would like to thank F. Kerr (General Manager), and J.L. Chakravatti (Environmental Engineer) of Denison Mines Ltd., for their great interest in this project. Thanks are also extended to C. Seeber (Denison Mines Ltd.) for providing data for this project.

REFERENCES

1. Bigu, J. and Grenier, M., "Studies of radioactive dust in Canadian uranium mines"; CIM Bull, vol. 77, No. 869, pp. 62-68, 1981.

2. Paschoa, A.S., Wrenn, M.E., Singh, N.P., Miller, S.C., Bruenger, K.W., Jones, K.W., Cholewa, M. and Hanson, A.L., "Uranium bearing particles in miner's and miller's lungs"; In: Occupational Radioactive Safety in Mining. (Toronto, Canada), Canadian Nuclear Association, pp. 511-517, 1984.

3. Duport, P.J. and Edwardson, E., "Determination of the contribution of long-lived dust to the committed dose equivalent received by uranium miners and mill workers in the Elliot Lake area"; Information Reports INFO-0167-1 and INFO-0167-2, Atomic Energy Control Board, Ottawa, 1985.

4. Bigu, J. and Grenier, M., "Characterization of radioactive dust in Canadian underground uranium mines"; Proc 2nd U.S. Mine Ventilation Symp; P. Mousset-Jones (Ed.), A.A. Balkema, Rotterdam/Boston, pp. 269-277, 1985.

5. Bigu, J., "Long-lived alpha-particle activity in dust samples from hard-rock uranium mines"; Am Ind Hyg Assoc J, vol. 49, No. 11, pp. 566-571, 1988.

6. Knight, G., "Detailed studies on the assessment of quartz by X-ray diffraction in airborne dust samples and their collection in hard-rock mines"; Division Report MRP/MRL 75-17(TR), CANMET, Energy, Mines and Resources Canada, 1975.

7. Bigu, J., "Alpha-particle activity associated with Long-Lived Radioactive Dust samples from an underground uranium mine"; Division Report MRL 90-31(TR), October 1989.

Table 1 - LLRD, respirable dust (RD) and silica dust (S_iO_2) data from Denison Mines Ltd.

S #	RD (ug)	SiO2 (ug)	Tri #	eff.	cpa (g)	B (cpa)	cpa(g)-B(cpa)	aBq	LLRD/SiO2 (aBq/ug)
1444	2.20	0.914	7	0.457	0.244	0.183	0.061	2.225	2.43
1445	0.30	0.017	8	0.470	0.200	0.086	0.114	4.043	237.80
1452	0.30	0.008	5	0.462	0.455	0.280	0.175	6.313	789.14
1453	0.30	0.022	6	0.463	0.177	0.166	0.011	0.396	18.00
1468	0.30	0.005	7	0.457	0.200	0.183	0.017	0.620	124.00
1474	0.30	0.014	9	0.458	0.188	0.093	0.095	3.457	246.93
1478	0.10	0.008	5	0.462	0.711	0.280	0.431	15.548	1943.54
1479	0.30	0.030	6	0.463	0.889	0.166	0.723	26.026	867.53
1485	0.10	0.008	7	0.457	0.733	0.183	0.550	20.058	2507.29
1494	0.30	0.008	9	0.458	0.822	0.093	0.729	26.528	3316.05
1495	0.20	0.007	4	0.461	0.300	0.133	0.167	6.038	862.51
1497	0.10	0.009	5	0.462	0.344	0.280	0.064	2.309	256.53
1499	0.10	0.052	6	0.463	0.655	0.166	0.489	17.603	338.51
1500	1.80	0.038	7	0.457	1.577	0.183	1.394	50.839	1337.86
1504	0.60	0.112	4	0.461	0.588	0.133	0.455	16.450	146.87
1506	0.60	0.023	5	0.462	0.622	0.280	0.342	12.338	536.42
1508	0.10	0.010	6	0.463	0.444	0.166	0.278	10.007	1000.72
1509	0.30	0.021	7	0.457	0.566	0.183	0.383	13.968	665.14
1510	1.00	0.117	9	0.458	0.611	0.093	0.518	18.850	161.11
1511	0.30	0.018	8	0.470	0.555	0.086	0.469	16.631	923.96
1512	0.10	0.012	9	0.458	0.300	0.093	0.207	7.533	627.73
1513	0.30	0.029	4	0.461	0.388	0.133	0.255	9.219	317.90
1514	0.10	0.085	5	0.462	0.744	0.280	0.464	16.739	196.93
1515	0.10	0.056	6	0.463	0.988	0.166	0.822	29.590	528.39
1516	0.20	0.045	7	0.457	0.722	0.183	0.539	19.657	436.83
1517	0.30	0.014	8	0.470	0.166	0.086	0.080	2.837	202.63
1519	0.40	0.073	4	0.461	0.788	0.133	0.655	23.680	324.39
1520	0.20	0.053	5	0.462	0.667	0.280	0.387	13.961	263.42
1521	0.20	0.037	6	0.463	0.644	0.166	0.478	17.207	465.04
1522	0.20	0.087	7	0.457	0.655	0.183	0.472	17.214	197.86
1523	0.10	0.007	8	0.470	0.133	0.086	0.047	1.667	238.10
1524	0.20	0.010	9	0.458	0.177	0.093	0.084	3.057	305.68
1525	0.40	0.013	4	0.461	0.322	0.133	0.189	6.833	525.61
1526	0.40	0.034	5	0.462	0.611	0.280	0.331	11.941	351.20
1527	0.30	0.010	6	0.463	0.255	0.166	0.089	3.204	320.37
1529	0.30	0.009	8	0.470	0.500	0.086	0.414	14.681	1631.21
1530	0.50	0.021	9	0.458	0.288	0.093	0.195	7.096	337.91
1531	0.20	6.461	4	0.461	0.288	0.133	0.155	5.604	0.87
1533	0.40	0.055	6	0.463	0.233	0.166	0.067	2.412	43.85
1536	0.20	0.011	9	0.458	0.100	0.093	0.007	0.255	23.16
1537	0.70	0.027	4	0.461	0.211	0.133	0.078	2.820	104.44
1540	0.90	0.012	7	0.457	0.277	0.183	0.094	3.428	285.68
1541	0.50	0.036	8	0.470	0.155	0.086	0.069	2.447	67.97
1544	0.10	0.007	5	0.462	0.322	0.280	0.042	1.515	216.45
1545	0.00	0.004	6	0.463	0.222	0.166	0.056	2.016	503.96
1547	0.10	0.012	8	0.470	0.444	0.086	0.358	12.695	1057.92
1551	1.00	0.008	5	0.462	0.377	0.280	0.097	3.499	437.41
1552	0.10	0.002	6	0.463	0.200	0.166	0.034	1.224	611.95
1554	0.10	0.006	8	0.470	1.000	0.086	0.914	32.411	5401.89
1555	0.10	0.032	9	0.458	1.155	0.093	1.062	38.646	1207.70
1556	0.00	0.013	4	0.461	1.022	0.133	0.889	32.140	2472.33
1557	0.10	0.058	5	0.462	1.177	0.280	0.897	32.359	557.92
1558	0.00	0.003	6	0.463	0.366	0.166	0.200	7.199	2399.81
1559	0.10	0.014	7	0.457	1.066	0.183	0.883	32.203	2300.20
1560	0.40	0.033	8	0.470	0.333	0.086	0.247	8.759	265.42

Cont.

Table 1 - cont.

S #	RD (ug)	SiO2 (ug)	Tri #	eff.	cpm (g)	B (cpm)	cpm(g)-B(cpm)	mBg	LLRD/SiO2 (mBg/ug)
1561	0.10	0.003	9	0.458	0.144	0.093	0.051	1.856	618.63
1562	0.30	0.019	4	0.461	0.266	0.133	0.133	4.808	253.07
1563	1.20	0.344	5	0.462	1.811	0.280	1.531	55.231	160.55
1564	0.40	0.018	6	0.463	0.288	0.166	0.122	4.392	243.98
1565	0.40	0.032	7	0.457	0.233	0.183	0.050	1.823	56.98
1566	0.40	0.049	8	0.470	0.211	0.086	0.125	4.433	90.46
1567	0.20	0.009	9	0.458	0.222	0.093	0.129	4.694	521.59
1569	0.80	0.015	5	0.462	0.422	0.280	0.142	5.123	341.51
1570	0.30	0.029	6	0.463	0.233	0.166	0.067	2.412	83.17
1571	0.10	0.021	7	0.457	0.344	0.183	0.161	5.872	279.60
1572	0.20	0.010	8	0.470	0.144	0.086	0.058	2.057	205.67
1573	0.10	0.008	9	0.458	0.100	0.093	0.007	0.255	31.84
1574	0.10	0.021	4	0.461	0.133	0.133	0.000	0.000	0.00
1576	0.30	0.012	6	0.463	0.222	0.166	0.056	2.016	167.99
1577	0.10	0.033	7	0.457	0.222	0.183	0.039	1.422	43.10
1578	0.10	0.010	8	0.470	0.222	0.086	0.136	4.823	482.27
1579	0.20	0.059	9	0.458	0.355	0.093	0.262	9.534	161.60
1580	0.10	0.032	4	0.461	0.166	0.133	0.033	1.193	37.28
1581	0.30	0.059	5	0.462	0.477	0.280	0.197	7.107	120.45
1582	0.00	0.006	4	0.461	0.144	0.133	0.011	0.398	66.28
1583	0.20	0.013	5	0.462	0.344	0.280	0.064	2.309	177.60
1585	0.30	0.043	7	0.457	0.366	0.183	0.183	6.674	155.21
1586	0.20	0.071	8	0.470	0.433	0.086	0.347	12.305	173.31
1587	0.10	0.010	9	0.458	0.100	0.093	0.007	0.255	25.47
1588	0.30	0.002	4	0.461	0.144	0.133	0.011	0.398	198.84
1589	0.40	0.028	5	0.462	0.322	0.280	0.042	1.515	54.11
1590	0.20	0.043	6	0.463	0.233	0.166	0.067	2.412	56.09
1592	0.10	0.010	8	0.470	0.255	0.086	0.169	5.993	599.29
1593	3.20	1.818	9	0.458	9.688	0.093	9.595	349.163	192.06
1595	0.10	0.053	5	0.462	0.933	0.280	0.653	23.557	444.47
1596	2.50	1.250	6	0.463	6.655	0.166	6.489	233.585	186.87
1598	0.20	0.006	8	0.470	0.133	0.086	0.047	1.667	277.78
1601	0.70	0.091	5	0.462	0.566	0.280	0.286	10.317	113.38
1602	0.30	0.026	6	0.463	0.277	0.166	0.111	3.996	153.68
1603	0.20	0.007	9	0.457	0.344	0.183	0.161	5.872	838.80
1604	0.30	0.006	8	0.470	0.222	0.086	0.136	4.823	803.78
1606	0.20	0.020	4	0.461	0.155	0.133	0.022	0.795	39.77
1608	0.00	0.020	6	0.463	1.022	0.166	0.856	30.814	1540.68
1609	0.00	0.008	7	0.457	0.389	0.183	0.205	7.476	934.54
1611	0.00	0.024	9	0.458	1.611	0.093	1.518	55.240	2301.67
1612	0.00	0.004	4	0.461	0.144	0.133	0.011	0.398	99.42
1617	0.00	0.011	9	0.458	0.233	0.093	0.140	5.095	463.15
1618	0.10	0.010	8	0.470	0.444	0.086	0.358	12.695	1269.50
1620	0.00	0.008	5	0.462	0.444	0.280	0.164	5.916	739.54
1621	0.00	0.012	6	0.463	0.277	0.166	0.111	3.996	332.97
1622	0.00	0.077	7	0.457	0.288	0.183	0.105	3.829	49.73
1623	0.00	0.018	8	0.470	0.144	0.086	0.058	2.057	114.26
1624	0.00	0.014	9	0.458	0.122	0.093	0.029	1.055	75.38
1625	0.00	0.014	4	0.461	0.266	0.133	0.133	4.808	343.46
1626	0.00	0.020	5	0.462	0.311	0.280	0.031	1.118	55.92
1627	0.20	0.013	6	0.463	0.277	0.166	0.111	3.996	307.36
1628	0.01	7.000	7	0.457	0.311	0.183	0.128	4.668	0.67
1629	0.20	0.009	8	0.470	0.300	0.086	0.214	7.589	843.18
1630	0.30	0.012	9	0.458	0.233	0.093	0.140	5.095	424.55
1631	0.30	0.075	4	0.461	0.388	0.133	0.255	9.219	122.92

Cont.

Table 1 - cont.

S #	RD (ag)	SiO2 (ag)	Tri #	eff.	cpm (g)	B (cpm)	cpm(g)-B(cpm)	mBq	LLRD/SiO2 (mBq/ag)
1632	0.90	0.096	5	0.462	0.877	0.280	0.597	21.537	224.34
1633	0.10	0.029	6	0.463	0.522	0.166	0.356	12.815	441.90
1634	0.10	0.016	7	0.457	0.244	0.183	0.061	2.225	139.04
1635	0.10	0.024	8	0.470	1.322	0.086	1.236	43.830	1826.24
1636	0.10	0.005	9	0.458	0.222	0.093	0.129	4.694	938.86
1637	0.20	0.045	4	0.461	1.277	0.133	1.144	41.359	919.10
1638	0.50	0.072	5	0.462	0.444	0.280	0.164	5.916	82.17
1639	0.30	0.015	6	0.463	0.667	0.166	0.501	18.035	1202.30
1640	0.30	0.009	7	0.457	0.577	0.183	0.394	14.369	1596.56
1642	0.20	0.013	9	0.458	0.200	0.093	0.107	3.894	299.52
1643	0.30	0.007	4	0.461	0.200	0.133	0.067	2.422	346.04
1645	0.50	0.006	6	0.463	0.188	0.166	0.022	0.792	131.99
1646	0.60	0.052	7	0.457	0.488	0.183	0.305	11.123	213.91
1647	0.20	0.012	8	0.470	0.222	0.086	0.136	4.823	401.89
1649	0.10	0.003	4	0.461	0.233	0.133	0.100	3.615	1205.11
1650	0.30	0.007	5	0.462	0.667	0.280	0.387	13.961	1994.43
1651	0.10	0.004	6	0.463	0.544	0.166	0.378	13.607	3401.73
1652	0.10	0.006	7	0.457	1.488	0.183	1.305	47.593	7932.17
1653	0.20	0.003	8	0.470	0.500	0.086	0.414	14.681	4893.62
1654	0.10	0.006	9	0.458	0.444	0.093	0.351	12.773	2128.82
1655	0.10	0.009	4	0.461	0.433	0.133	0.300	10.846	1205.11
1656	0.20	0.006	5	0.462	0.588	0.280	0.308	11.111	1851.85
1657	0.30	0.004	6	0.463	0.344	0.166	0.178	6.407	1601.87
1658	0.10	0.007	7	0.457	0.288	0.183	0.105	3.829	547.05
1659	0.20	0.007	9	0.458	0.333	0.133	0.200	7.278	1039.72
1679	0.00	0.019	5	0.462	0.444	0.280	0.164	5.916	311.38
1680	0.00	0.011	6	0.463	0.177	0.166	0.011	0.396	36.00
1681	0.00	0.058	7	0.457	0.488	0.183	0.305	11.123	191.78
1682	0.00	0.007	8	0.470	0.211	0.086	0.125	4.433	633.23
1683	0.00	0.056	9	0.458	0.144	0.093	0.051	1.856	33.14
1684	0.00	0.003	4	0.461	0.222	0.133	0.089	3.218	1072.55
1685	0.00	0.017	5	0.462	0.544	0.280	0.264	9.524	560.22
1686	0.00	0.005	6	0.463	0.188	0.166	0.022	0.792	158.39
1687	0.00	0.047	7	0.457	0.344	0.183	0.161	5.872	124.93
1689	0.00	0.003	9	0.458	0.122	0.093	0.029	1.055	351.77
1690	0.00	0.022	4	0.461	0.166	0.133	0.033	1.193	54.23
1691	0.00	0.005	5	0.462	0.400	0.280	0.120	4.329	865.80
1692	0.00	0.056	6	0.463	0.244	0.166	0.078	2.808	50.14
1693	0.00	0.003	7	0.457	0.255	0.183	0.072	2.626	875.27
1694	0.50	0.052	8	0.470	0.288	0.086	0.202	7.163	137.75
1695	0.20	0.007	9	0.458	0.200	0.093	0.107	3.894	556.25
1696	0.10	0.011	4	0.461	0.233	0.133	0.100	3.615	328.67
1697	1.00	0.222	5	0.462	1.300	0.280	1.020	36.797	165.75
1698	0.30	0.016	6	0.463	0.288	0.166	0.122	4.392	274.48
1699	0.40	0.037	7	0.457	0.211	0.183	0.028	1.021	27.60
1704	0.30	0.006	6	0.463	0.233	0.166	0.067	2.412	401.97
1705	0.30	0.037	7	0.457	0.333	0.183	0.150	5.470	147.85
1707	0.60	0.014	8	0.470	0.288	0.086	0.202	7.163	511.65
1708	0.10	0.003	6	0.463	0.188	0.166	0.022	0.792	263.98
1725	0.10	0.029	8	0.470	0.177	0.086	0.091	3.227	111.27
1726	0.00	0.003	9	0.458	0.100	0.093	0.007	0.255	84.91
1732	0.10	0.006	9	0.458	0.122	0.093	0.029	1.055	175.89
1733	0.10	0.005	4	0.461	0.144	0.133	0.011	0.398	79.54
1735	0.60	0.077	6	0.463	0.255	0.166	0.089	3.204	41.61
1737	0.50	0.047	8	0.470	0.233	0.086	0.147	5.213	110.91

Cont.

Table 1 - cont.

S #	RD (ag)	SiO2 (ag)	Tri #	eff.	cpa (g)	B (cpa)	cpa(g)-B(cpa)	aBg	LLRD/SiO2 (aBg/ag)
1738	0.20	0.016	9	0.458	0.122	0.093	0.029	1.055	65.96
1739	0.20	0.025	4	0.461	0.133	0.133	0.000	0.000	0.00
1743	0.20	0.052	8	0.470	0.177	0.086	0.091	3.227	62.06
1744	0.10	0.006	9	0.458	0.100	0.093	0.007	0.255	42.46
1745	0.40	0.005	4	0.461	0.177	0.133	0.044	1.591	318.15
1746	0.20	0.004	5	0.462	0.377	0.280	0.097	3.499	874.82
1747	0.20	0.001	6	0.463	0.355	0.166	0.189	6.803	6803.46
1748	0.20	0.014	7	0.457	0.288	0.183	0.105	3.829	273.52
1761	0.20	0.028	8	0.470	0.144	0.086	0.058	2.057	73.45
1762	0.10	0.028	9	0.458	0.166	0.093	0.073	2.656	94.87
1763	0.40	0.016	4	0.461	0.244	0.133	0.111	4.013	250.81
1764	0.40	0.037	5	0.462	0.355	0.280	0.075	2.706	73.13
1766	0.30	0.006	7	0.457	0.211	0.183	0.028	1.021	170.19
1767	0.60	0.033	8	0.470	0.222	0.086	0.136	4.823	146.14
1768	0.30	0.016	9	0.458	0.200	0.093	0.107	3.894	243.36
1776	0.10	0.006	4	0.461	0.166	0.133	0.033	1.193	198.84
1777	0.10	0.010	5	0.462	0.322	0.280	0.042	1.515	151.52
1778	0.40	0.006	6	0.463	0.244	0.166	0.078	2.808	467.96
1780	0.50	0.033	8	0.470	0.144	0.086	0.058	2.057	62.33
1781	0.20	0.008	9	0.458	0.233	0.093	0.140	5.095	636.83
1782	0.10	0.005	4	0.461	0.155	0.133	0.022	0.795	159.07
1783	0.20	0.021	5	0.462	0.288	0.280	0.008	0.289	13.74
1784	0.30	0.013	6	0.463	0.177	0.166	0.011	0.396	30.46
1785	0.10	0.026	7	0.457	0.244	0.183	0.061	2.225	85.56
1790	0.20	0.019	4	0.461	0.355	0.133	0.222	8.026	422.42
1792	0.50	0.111	6	0.463	0.722	0.166	0.556	20.014	180.31
1793	0.10	0.021	7	0.457	0.655	0.183	0.472	17.214	819.70
1794	1.20	0.373	8	0.470	1.656	0.086	1.570	55.674	149.26
1795	0.20	0.072	9	0.458	0.222	0.093	0.129	4.694	65.20
1796	0.40	0.008	4	0.461	0.155	0.133	0.022	0.795	99.42
1798	0.40	0.017	6	0.463	0.166	0.166	0.000	0.000	0.00
1800	0.30	0.040	8	0.470	0.255	0.086	0.169	5.993	149.82
1801	0.30	0.028	9	0.458	0.311	0.093	0.218	7.933	283.32
1802	0.40	0.092	4	0.461	0.422	0.133	0.289	10.448	113.57
1803	0.50	0.030	5	0.462	0.488	0.280	0.208	7.504	250.12
1804	0.60	0.155	6	0.463	0.667	0.166	0.501	18.035	116.35
1806	0.10	0.003	8	0.470	0.177	0.086	0.091	3.227	1075.65
1812	0.10	0.003	7	0.457	0.200	0.183	0.017	0.620	206.66
1813	0.30	0.047	8	0.470	0.277	0.086	0.191	6.773	144.11
1814	0.20	0.006	9	0.458	0.222	0.093	0.129	4.694	782.39
1818	0.20	0.072	6	0.463	0.622	0.166	0.456	16.415	227.98
1819	0.20	0.007	7	0.457	0.300	0.183	0.117	4.267	609.57
1821	0.60	0.024	9	0.458	0.655	0.093	0.562	20.451	852.13
1822	0.30	0.028	4	0.461	0.288	0.133	0.155	5.604	200.13
1824	0.00	0.005	5	0.462	0.411	0.280	0.131	4.726	945.17
1827	0.10	0.004	8	0.470	0.780	0.086	0.694	24.610	6152.48
1828	0.20	0.027	9	0.458	0.733	0.093	0.640	23.290	862.58
1829	0.10	0.019	4	0.461	0.277	0.133	0.144	5.206	274.00
1830	0.30	0.026	5	0.462	0.411	0.280	0.131	4.726	181.76
1831	0.20	0.025	6	0.463	0.244	0.166	0.078	2.808	112.31
1832	0.20	0.042	7	0.457	0.233	0.183	0.050	1.823	43.42
1833	0.50	0.107	8	0.470	0.255	0.086	0.169	5.993	56.01
1834	0.90	0.107	9	0.458	0.411	0.093	0.318	11.572	108.15
1835	0.40	0.050	4	0.461	0.766	0.133	0.133	4.808	96.17
1836	0.30	0.032	5	0.462	0.333	0.280	0.053	1.912	59.75

Cont.

Table 1 - cont.

S #	RD (ag)	SiO2 (ag)	Tri #	eff.	cpa (g)	B (cpa)	cpa(g)-B(cpa)	aBq	LLRD/SiO2 (aBq/ag)
1838	0.30	0.063	7	0.457	0.466	0.183	0.283	10.321	163.82
1839	0.50	0.050	8	0.470	0.266	0.086	0.180	6.383	127.66
1840	0.10	0.008	9	0.458	0.311	0.093	0.218	7.933	991.63
1841	0.20	0.022	4	0.461	0.322	0.133	0.189	6.833	310.59
1842	0.10	0.008	5	0.462	0.311	0.280	0.031	1.118	139.79
1843	0.20	0.008	6	0.463	3.222	0.166	3.056	110.007	13750.90
1845	0.10	0.024	8	0.470	0.700	0.086	0.614	21.773	907.21
1846	0.10	0.006	9	0.458	0.244	0.093	0.151	5.495	915.82
1847	0.80	0.145	4	0.461	0.933	0.133	0.800	28.923	199.47
1848	0.70	0.037	5	0.462	0.588	0.280	0.308	11.111	300.30
1849	0.10	0.007	6	0.463	0.188	0.166	0.022	0.792	113.13
1850	0.10	0.006	7	0.457	0.211	0.183	0.028	1.021	170.19
1851	3.90	1.202	8	0.470	5.611	0.086	5.525	195.922	163.00
1852	0.50	0.031	9	0.458	0.144	0.093	0.051	1.856	59.87
1854	0.01	0.004	5	0.462	0.355	0.280	0.075	2.706	676.41
1887	0.10	0.022	6	0.463	0.277	0.166	0.111	3.996	181.62
1888	0.50	0.039	7	0.457	0.222	0.183	0.039	1.422	36.47
1889	0.10	0.011	8	0.470	0.188	0.086	0.102	3.617	328.82
1890	0.40	0.007	9	0.458	0.144	0.093	0.051	1.856	265.13
1891	0.40	0.071	4	0.461	0.400	0.133	0.267	9.653	135.96
1893	0.90	0.277	6	0.463	2.011	0.166	1.845	66.415	239.76
1894	0.10	0.033	7	0.457	0.333	0.183	0.150	5.470	165.77
1895	0.60	0.104	8	0.470	0.988	0.086	0.902	31.986	307.56
1896	0.30	0.027	9	0.458	0.266	0.093	0.173	6.295	233.17
1897	1.40	0.005	4	0.461	0.244	0.133	0.111	4.013	802.60
1898	0.10	0.013	5	0.462	0.288	0.280	0.008	0.289	22.20
1899	0.30	0.070	6	0.463	0.500	0.166	0.334	12.023	171.76
1900	0.70	0.115	7	0.457	0.777	0.183	0.594	21.663	188.37
1901	0.20	0.017	8	0.470	0.277	0.086	0.191	6.773	398.41
1902	0.10	0.018	9	0.458	0.255	0.093	0.162	5.895	327.51
1903	0.30	0.018	4	0.461	0.566	0.133	0.433	15.654	869.69
1904	0.00	0.007	5	0.462	0.411	0.280	0.131	4.726	675.12
1922	0.01	0.009	9	0.458	0.166	0.093	0.073	2.656	295.16
1924	0.01	0.002	5	0.462	0.333	0.280	0.053	1.912	955.99
1926	0.01	0.003	7	0.457	0.244	0.183	0.061	2.225	741.55
1927	0.20	0.004	8	0.470	0.188	0.086	0.102	3.617	904.26
1928	0.60	0.063	9	0.458	0.577	0.093	0.484	17.613	279.57
1929	0.60	0.003	4	0.461	0.222	0.133	0.089	3.218	1072.55
1932	0.40	0.009	7	0.222	0.222	0.183	0.039	2.928	325.33
1933	0.10	0.023	8	0.470	0.255	0.086	0.169	5.993	260.56
1934	0.01	0.001	9	0.458	0.155	0.093	0.062	2.256	2256.19
1935	0.20	0.002	4	0.461	0.177	0.133	0.044	1.591	795.37
1936	0.20	0.007	5	0.462	0.288	0.280	0.008	0.289	41.23
1937	0.01	0.005	6	0.463	0.200	0.166	0.034	1.224	244.78
1938	0.20	0.030	7	0.457	0.277	0.183	0.094	3.428	114.27
1939	0.10	0.002	8	0.470	0.133	0.086	0.047	1.667	833.33
1940	0.10	0.008	9	0.458	0.166	0.093	0.073	2.656	332.06
1941	0.50	0.010	4	0.461	0.244	0.133	0.111	4.013	401.30
1942	0.40	0.015	5	0.462	0.300	0.280	0.020	0.722	48.10
1943	1.00	0.018	6	0.463	0.188	0.166	0.022	0.792	44.00
1944	0.10	0.006	7	0.457	0.188	0.183	0.005	0.182	30.39
1945	0.20	0.014	8	0.470	0.177	0.086	0.091	3.227	230.50
1946	0.10	0.017	9	0.458	0.211	0.093	0.118	4.294	252.59
1947	0.00	0.049	4	0.461	0.577	0.133	0.444	16.052	327.59
1948	0.00	0.021	5	0.462	0.433	0.280	0.153	5.519	262.83

Cont.

Table 1 - cont.

S #	RD (mg)	SiO2 (mg)	Tri #	eff.	cpm (g)	B (cpm)	cpm(g)-B(cpm)	mBq	LLRD/SiO2 (mBq/mg)
1949	0.00	0.039	6	0.463	0.322	0.166	0.156	5.616	143.99
1951	0.00	0.009	8	0.470	0.188	0.086	0.102	3.617	401.89
1952	0.00	0.044	9	0.458	0.411	0.093	0.318	11.572	263.00
1953	0.00	0.025	4	0.461	0.388	0.133	0.255	9.219	368.76
1954	0.00	0.027	5	0.462	0.466	0.280	0.186	6.710	248.52
1955	0.00	0.027	6	0.463	0.277	0.166	0.111	3.996	147.99
1956	0.00	0.008	7	0.457	0.400	0.183	0.217	7.914	989.24
1957	0.00	0.007	8	0.470	0.333	0.086	0.247	8.759	1251.27
1958	0.00	0.028	9	0.458	0.244	0.093	0.151	5.495	196.25
1959	0.00	1.245	4	0.461	3.000	0.133	2.867	103.651	83.25
1960	0.00	0.008	5	0.462	0.422	0.280	0.142	5.123	640.33
1961	0.00	0.088	6	0.463	0.577	0.166	0.411	14.795	168.12
1962	0.00	0.003	7	0.457	0.322	0.183	0.139	5.069	1689.76
1963	0.00	0.004	8	0.470	0.111	0.086	0.025	0.887	221.63
1964	0.00	0.005	9	0.458	0.100	0.093	0.007	0.255	50.95
1965	0.00	0.018	4	0.461	0.900	0.133	0.767	27.730	1540.53
1966	0.00	0.015	5	0.462	0.744	0.280	0.464	16.739	1115.92
1967	0.00	0.079	6	0.463	0.555	0.166	0.389	14.003	177.25
1968	0.00	0.126	7	0.457	0.755	0.183	0.572	20.861	165.56
1969	0.00	0.024	8	0.470	0.222	0.086	0.136	4.823	200.95
1970	0.00	0.008	9	0.458	1.188	0.093	1.095	39.847	4980.90
1971	0.00	0.015	4	0.461	0.344	0.133	0.211	7.628	508.56
1972	0.00	0.011	5	0.462	0.400	0.280	0.120	4.329	393.55
1973	0.00	0.018	6	0.463	0.244	0.166	0.078	2.808	155.99
1975	0.00	0.009	8	0.470	0.188	0.086	0.102	3.617	401.89
1976	0.00	0.007	9	0.458	0.188	0.093	0.095	3.457	493.87
1978	0.01	0.027	5	0.462	0.366	0.280	0.086	3.102	114.91
1979	0.02	0.086	6	0.463	0.777	0.166	0.611	21.994	255.75
1981	0.01	0.061	8	0.470	0.177	0.086	0.091	3.227	52.90
1982	0.01	0.004	9	0.458	0.233	0.093	0.140	5.095	1273.65
1985	0.03	0.005	6	0.463	0.288	0.166	0.122	4.392	878.33
1986	0.01	0.014	7	0.457	0.244	0.183	0.061	2.225	158.90
1988	0.02	0.006	9	0.458	0.200	0.093	0.107	3.894	648.96
1989	0.01	0.003	4	0.461	0.244	0.133	0.111	4.013	1337.67
1990	0.30	0.055	5	0.462	0.344	0.280	0.064	2.309	41.98
1991	0.10	0.005	6	0.463	0.166	0.166	0.000	0.000	0.00
1992	0.20	0.046	7	0.457	0.255	0.183	0.072	2.626	57.08
1995	0.10	0.025	9	0.458	0.133	0.093	0.040	1.456	58.22
1996	0.10	0.031	4	0.461	0.266	0.133	0.133	4.808	155.11
1997	0.10	0.009	5	0.462	0.288	0.280	0.008	0.289	32.07
1998	0.10	0.040	6	0.463	0.377	0.166	0.211	7.595	189.88
2000	0.30	0.051	8	0.470	0.144	0.086	0.058	2.057	40.33
2001	0.10	0.026	9	0.458	0.133	0.093	0.040	1.456	55.98
2002	0.70	0.093	4	0.461	0.400	0.133	0.267	9.653	103.79
2003	0.01	0.006	5	0.462	0.288	0.280	0.008	0.289	48.10
2004	0.50	0.220	6	0.463	1.088	0.166	0.922	33.189	150.86
2005	0.01	0.009	7	0.457	0.188	0.183	0.005	0.182	20.26
2006	0.01	0.007	8	0.470	0.122	0.086	0.036	1.277	182.37
2009	0.30	0.041	5	0.462	0.522	0.280	0.242	8.730	212.93
2010	0.10	0.012	6	0.463	0.233	0.166	0.067	2.412	200.98
2012	0.10	0.048	8	0.470	0.433	0.086	0.347	12.305	256.35
2013	0.10	0.009	9	0.458	0.100	0.093	0.007	0.255	28.30
2016	0.00	0.001	6	0.463	0.322	0.166	0.156	5.616	5615.55
2018	0.00	0.009	8	0.470	0.166	0.086	0.080	2.837	315.21
2019	0.40	0.045	9	0.458	0.688	0.093	0.595	21.652	481.16

Cont.

Table 1 - cont.

S #	RD (ug)	SiO2 (ug)	Tri #	eff.	cpm (g)	B (cpm)	cpm(g)-B(cpm)	mBq	LLRD/SiO2 (mBq/ug)
2020	0.00	0.010	4	0.461	0.244	0.133	0.111	4.013	401.30
2021	0.20	0.005	5	0.462	0.800	0.280	0.520	18.759	3751.80
2022	0.30	0.004	6	0.463	0.311	0.166	0.145	5.220	1304.90
2023	0.20	0.019	7	0.457	0.411	0.183	0.228	8.315	437.64
2024	0.40	0.068	8	0.470	0.866	0.086	0.780	27.660	406.76
2025	0.10	0.007	9	0.458	0.466	0.093	0.373	13.574	1939.07
2031	0.00	0.013	9	0.458	0.200	0.093	0.107	3.894	299.52
2033	0.00	0.003	5	0.462	0.322	0.280	0.042	1.515	505.05
2035	0.40	0.195	7	0.457	0.833	0.183	0.650	23.705	121.57
2036	0.10	0.008	8	0.470	0.200	0.086	0.114	4.043	505.32
2037	0.40	0.007	9	0.458	0.133	0.093	0.040	1.456	207.94
2039	0.20	0.029	5	0.462	0.366	0.280	0.086	3.102	106.98
2040	0.00	0.005	6	0.463	0.200	0.166	0.034	1.224	244.78
2042	0.00	0.004	8	0.470	0.111	0.086	0.025	0.887	221.63
2043	0.50	0.109	9	0.458	1.222	0.093	1.129	41.084	376.92
2044	0.80	0.008	4	0.461	0.266	0.133	0.133	4.808	601.05
2051	0.60	0.003	5	0.462	0.577	0.280	0.297	10.714	3571.43
2053	0.00	0.004	7	0.457	0.222	0.183	0.039	1.422	355.58
2055	0.20	0.041	9	0.458	0.166	0.093	0.073	2.656	64.79
2056	0.30	0.016	4	0.461	0.233	0.133	0.100	3.615	225.96
2060	0.50	0.273	8	0.470	2.422	0.086	2.336	82.837	303.43
2061	0.20	0.072	9	0.458	0.155	0.093	0.062	2.256	31.34
2064	0.00	0.028	5	0.462	0.400	0.280	0.120	4.329	154.61
2065	0.00	0.008	6	0.463	0.933	0.166	0.767	27.610	3451.22
2066	0.00	0.006	7	0.457	0.677	0.183	0.494	18.016	3002.67
2067	0.00	0.021	8	0.470	1.000	0.086	0.914	32.411	1543.40
2069	0.00	0.009	4	0.461	0.322	0.133	0.189	6.833	759.22
2070	0.00	0.002	5	0.462	0.622	0.280	0.342	12.338	6168.83
2074	0.00	0.008	9	0.458	0.122	0.093	0.029	1.055	131.91
2076	0.00	0.006	5	0.462	0.311	0.280	0.031	1.118	186.39
2077	0.00	0.008	6	0.463	0.177	0.166	0.011	0.396	49.50
2079	0.00	0.028	8	0.470	0.100	0.086	0.014	0.496	17.73
2080	0.00	0.027	9	0.458	0.200	0.093	0.107	3.894	144.21
2081	0.00	0.022	4	0.461	0.200	0.133	0.067	2.422	110.10
2082	0.00	0.022	5	0.462	0.377	0.280	0.097	3.499	159.06
2083	0.00	0.086	6	0.463	0.311	0.166	0.145	5.220	60.69
2084	0.00	0.027	7	0.457	0.222	0.183	0.039	1.422	52.68
2085	0.00	0.010	8	0.470	0.111	0.086	0.025	0.887	88.65
2087	0.00	0.014	4	0.461	0.233	0.133	0.100	3.615	258.24
2088	0.00	0.018	5	0.462	0.333	0.280	0.053	1.912	106.22
2091	0.00	0.007	8	0.470	0.088	0.086	0.002	0.071	10.13
2092	0.00	0.008	9	0.458	0.166	0.093	0.073	2.656	332.06
2095	0.00	0.039	6	0.463	0.211	0.166	0.045	1.620	41.54
2099	0.00	0.006	4	0.461	0.222	0.133	0.089	3.218	536.27
2102	0.00	0.005	7	0.457	0.188	0.183	0.005	0.182	36.47
2103	0.50	0.021	8	0.470	0.088	0.086	0.002	0.071	3.38
2104	0.30	0.006	9	0.458	0.111	0.093	0.018	0.655	109.17
2105	0.80	0.152	4	0.461	0.144	0.133	0.011	0.398	2.62
2106	0.20	0.004	5	0.462	1.077	0.280	0.797	28.752	7187.95
2107	0.20	0.023	6	0.463	0.200	0.166	0.034	1.224	53.21
2108	0.20	0.007	7	0.457	0.222	0.183	0.039	1.422	203.19
2109	0.70	0.046	8	0.470	0.133	0.086	0.047	1.667	36.23
2110	0.20	0.009	9	0.458	0.188	0.093	0.095	3.457	384.12
2111	0.40	0.016	4	0.461	0.133	0.133	0.000	0.000	0.00
2112	1.30	0.215	5	0.462	0.322	0.280	0.042	1.515	7.05

Cont.

Table 1 - cont.

S #	RD (ag)	SiO2 (ng)	Tri #	eff.	cpm (g)	B (cpm)	cpm(g)-B(cpm)	aBq	LLRD/SiO2 (aBq/ng)
2113	0.40	0.016	6	0.463	0.811	0.166	0.645	23.218	1451.13
2114	0.70	0.016	7	0.457	0.288	0.183	0.105	3.829	239.33
2115	0.30	0.043	8	0.470	0.255	0.086	0.169	5.993	139.37
2116	0.20	0.006	9	0.458	0.233	0.093	0.140	5.095	849.10
2118	0.40	0.030	5	0.462	0.411	0.280	0.131	4.726	157.53
2119	0.00	0.008	6	0.463	0.166	0.166	0.000	0.000	0.00
2120	0.00	0.007	7	0.457	0.188	0.183	0.005	0.182	26.05
2121	0.10	0.015	8	0.470	0.311	0.086	0.225	7.979	531.91
2122	0.10	0.007	9	0.458	0.466	0.093	0.373	13.574	1939.07
2123	0.30	0.026	4	0.461	0.377	0.133	0.244	8.821	339.28
2125	0.10	0.017	6	0.463	0.366	0.166	0.200	7.199	423.50
2127	0.10	0.009	8	0.470	0.133	0.086	0.047	1.667	185.19
2128	0.20	0.008	9	0.458	0.144	0.093	0.051	1.856	231.99
2130	0.20	0.036	5	0.462	0.466	0.280	0.186	6.710	186.39
2131	0.20	0.008	6	0.463	0.211	0.166	0.045	1.620	202.48
2133	0.30	0.012	8	0.470	0.144	0.086	0.058	2.057	171.39
2134	0.20	0.041	9	0.458	0.200	0.093	0.107	3.894	94.97
2135	0.10	0.041	4	0.461	0.266	0.133	0.133	4.808	117.28
2137	1.10	0.138	6	0.463	0.577	0.166	0.411	14.795	107.21
2138	0.30	0.102	7	0.457	0.444	0.183	0.261	9.519	93.32
2139	0.40	0.244	8	0.470	1.400	0.086	1.314	46.596	190.97
2140	0.90	0.152	9	0.458	1.500	0.093	1.407	51.201	336.85
2141	0.80	0.608	4	0.461	2.822	0.133	2.689	97.216	159.90
2142	0.30	0.235	5	0.462	1.644	0.280	1.364	49.206	209.39
2143	0.20	0.050	6	0.463	0.444	0.166	0.278	10.007	200.14
2144	0.60	0.381	7	0.457	1.933	0.183	1.750	63.822	167.51
2145	2.50	0.216	8	0.470	1.888	0.086	1.802	63.901	295.84
2146	0.90	0.278	9	0.458	1.766	0.093	1.673	60.881	219.00
2147	1.00	0.256	4	0.461	1.722	0.133	1.589	57.448	224.40
2148	0.70	0.160	5	0.462	1.600	0.280	1.320	47.619	297.62
2151	0.00	0.003	8	0.470	0.122	0.086	0.036	1.277	425.53
2152	0.60	0.032	9	0.458	0.244	0.093	0.151	5.495	171.72
2155	0.10	0.003	6	0.463	0.188	0.166	0.022	0.792	263.98
2160	0.20	0.001	5	0.462	0.377	0.280	0.097	3.499	3499.28
2165	0.60	0.038	4	0.461	0.277	0.133	0.144	5.206	137.00
2167	0.20	0.009	6	0.463	0.266	0.166	0.100	3.600	399.97
2168	0.40	0.015	7	0.457	0.344	0.183	0.161	5.872	391.44
2169	0.00	0.018	8	0.470	0.255	0.086	0.169	5.993	332.94
2170	0.40	0.022	9	0.458	0.288	0.093	0.195	7.096	322.55
2171	0.50	0.019	4	0.461	0.222	0.133	0.089	3.218	169.35
2172	0.60	0.057	5	0.462	0.488	0.280	0.208	7.504	131.64
2174	0.20	0.007	7	0.457	0.244	0.183	0.061	2.225	317.81
2179	0.00	0.011	6	0.463	0.177	0.166	0.011	0.396	36.00
2181	0.00	0.006	8	0.470	0.144	0.086	0.058	2.057	342.79
2182	0.20	0.179	9	0.458	0.633	0.093	0.540	19.651	109.78
2183	0.00	0.003	4	0.461	0.177	0.133	0.044	1.591	530.25
2184	0.40	0.095	5	0.462	0.611	0.280	0.331	11.941	125.69
2186	0.30	0.011	7	0.457	0.255	0.183	0.072	2.626	238.71
2187	0.20	0.005	8	0.470	0.122	0.086	0.036	1.277	255.32
2188	0.40	0.013	9	0.458	0.100	0.093	0.007	0.255	19.59
2189	0.20	0.023	4	0.461	0.266	0.133	0.133	4.808	209.06
2191	0.10	0.004	6	0.463	0.200	0.166	0.034	1.224	305.98
2192	0.70	0.161	7	0.457	0.400	0.183	0.217	7.914	49.15
2193	0.60	0.007	8	0.470	0.155	0.086	0.069	2.447	349.54
2194	0.30	0.027	9	0.458	0.511	0.093	0.418	15.211	563.37

Cont.

Table - 1 cont.

S #	RD (ag)	SiO2 (ag)	Tri #	eff.	cpm (g)	B (cpm)	cpm(g)-B(cpm)	mBg	LLRD/SiO2 (mBg/ag)
2195	1.10	0.048	4	0.461	0.322	0.133	0.189	6.833	142.35
2196	0.70	0.040	5	0.462	0.677	0.280	0.397	14.322	358.04
2197	0.30	0.027	6	0.463	0.322	0.166	0.156	5.616	207.98
2198	0.50	0.006	7	0.457	0.200	0.183	0.017	0.620	103.33
2199	0.50	0.083	8	0.470	0.611	0.086	0.525	18.617	224.30
2201	0.90	0.046	4	0.461	0.444	0.133	0.311	11.244	244.43
2202	0.70	0.182	5	0.462	1.022	0.280	0.742	26.768	147.08
2203	0.90	0.092	6	0.463	1.077	0.166	0.911	32.793	356.45
2205	0.20	0.003	4	0.461	0.144	0.133	0.011	0.398	132.56
2206	0.30	0.008	5	0.462	0.377	0.280	0.097	3.499	437.41
2207	0.60	0.048	6	0.463	0.322	0.166	0.156	5.616	116.99
2208	0.10	0.007	7	0.457	0.277	0.183	0.094	3.428	489.74
2209	0.10	0.034	8	0.470	0.144	0.086	0.058	2.057	60.49
2214	0.50	0.014	4	0.461	0.155	0.133	0.022	0.795	56.81
2216	0.10	0.009	5	0.462	0.355	0.280	0.075	2.706	300.63
2217	0.40	0.004	6	0.463	0.211	0.166	0.045	1.620	404.97
2218	0.30	0.009	7	0.457	0.288	0.183	0.105	3.829	425.48
2219	0.20	0.009	8	0.470	0.100	0.086	0.014	0.496	55.16
2220	0.70	0.122	9	0.458	0.200	0.093	0.107	3.894	31.92
2222	0.10	0.011	4	0.461	0.255	0.133	0.122	4.411	400.97
2225	0.20	0.083	7	0.457	0.466	0.183	0.283	10.321	124.35
2226	0.30	0.030	8	0.470	0.133	0.086	0.047	1.667	55.56
2227	0.70	0.130	9	0.458	0.211	0.093	0.118	4.294	33.03
2228	0.20	0.036	4	0.461	0.233	0.133	0.100	3.615	100.43
2231	0.10	0.002	6	0.463	0.233	0.166	0.067	2.412	1205.90
2233	0.00	0.005	8	0.470	0.122	0.086	0.036	1.277	255.32
2234	0.00	0.016	9	0.458	0.122	0.093	0.029	1.055	65.96
2236	0.00	0.005	5	0.462	0.344	0.280	0.064	2.309	461.76
2237	0.00	0.006	4	0.461	0.333	0.133	0.200	7.231	1205.11
2238	0.20	0.008	5	0.462	0.300	0.280	0.020	0.722	90.19
2240	0.00	0.007	7	0.457	0.188	0.183	0.005	0.182	26.05
2241	0.20	0.041	4	0.461	0.277	0.133	0.144	5.206	126.98
2242	0.00	0.007	5	0.280	0.477	0.280	0.197	11.726	1675.17
2243	0.00	0.036	6	0.463	0.500	0.166	0.334	12.023	333.97
2244	0.00	0.012	7	0.457	0.500	0.183	0.317	11.561	963.41
2246	0.00	0.022	9	0.458	0.333	0.093	0.240	8.734	396.98
2247	0.00	0.004	4	0.461	0.144	0.133	0.011	0.398	99.42
2249	0.30	0.059	5	0.462	0.611	0.280	0.331	11.941	202.39
2250	0.00	0.023	6	0.463	0.277	0.166	0.111	3.996	173.73
2252	0.00	0.007	8	0.470	0.200	0.086	0.114	4.043	577.51
2280	0.00	0.004	4	0.461	0.155	0.133	0.022	0.795	198.84
2281	0.11	0.060	6	0.463	0.288	0.166	0.122	4.392	73.19
2282	0.11	0.023	7	0.457	0.488	0.183	0.305	11.123	483.62
2285	0.10	0.022	4	0.461	0.266	0.133	0.133	4.808	218.56
2286	0.40	0.180	5	0.462	0.522	0.280	0.242	8.730	48.50
2287	1.20	0.371	6	0.463	1.544	0.166	1.378	49.604	133.70
2289	0.50	0.055	8	0.470	0.411	0.086	0.325	11.525	209.54
2290	0.60	0.050	9	0.458	0.422	0.093	0.329	11.972	239.45
2293	0.20	0.015	4	0.461	0.533	0.133	0.400	14.461	964.09
2294	0.10	0.002	5	0.462	0.311	0.280	0.031	1.118	559.16
2296	0.12	0.148	5	0.462	0.533	0.280	0.253	9.127	61.67
2297	0.12	0.055	6	0.463	0.388	0.166	0.222	7.991	145.30
2298	0.11	0.052	7	0.457	0.333	0.183	0.150	5.470	105.20
2299	0.12	0.010	8	0.470	0.188	0.086	0.102	3.617	361.70
2302	0.11	0.006	5	0.462	0.588	0.280	0.308	11.111	1851.85

Cont.

Table 1 - cont.

S #	RD (ag)	SiO2 (ag)	Tri #	eff.	cpm (g)	B (cpm)	cpm(g)-B(cpm)	mBg	LLRD/SiO2 (mBg/ag)
2303	0.11	0.008	6	0.463	0.288	0.166	0.122	4.392	548.96
2304	0.12	0.023	7	0.457	0.277	0.183	0.094	3.428	149.05
2305	0.12	0.047	8	0.470	0.233	0.086	0.147	5.213	110.91
2306	0.12	0.038	9	0.458	0.255	0.093	0.162	5.895	155.14
2308	0.13	0.004	5	0.462	0.355	0.280	0.075	2.706	676.41
2309	0.13	0.007	6	0.463	0.288	0.166	0.122	4.392	627.38
2310	0.11	0.073	7	0.457	0.422	0.183	0.239	8.716	119.40
2311	0.12	0.018	8	0.470	0.255	0.086	0.169	5.993	332.94
2312	0.12	0.016	9	0.462	0.266	0.093	0.173	6.241	390.06
2313	0.12	0.014	4	0.461	0.222	0.133	0.089	3.218	229.83
2314	0.12	0.028	5	0.462	0.455	0.280	0.175	6.313	225.47
2315	0.12	0.009	6	0.463	0.200	0.166	0.034	1.224	135.99
2317	0.12	0.043	8	0.470	0.188	0.086	0.102	3.617	84.12
2318	0.11	0.118	9	0.458	0.444	0.093	0.351	12.773	108.25
2319	0.13	0.023	4	0.461	0.366	0.133	0.233	8.424	366.25
2320	0.12	0.055	5	0.462	0.411	0.280	0.131	4.726	85.92
2321	0.13	0.065	6	0.463	0.333	0.166	0.167	6.012	92.48
2324	0.30	0.006	9	0.458	0.155	0.093	0.062	2.256	376.03
2325	0.20	0.009	4	0.461	0.222	0.133	0.089	3.218	357.52
2328	0.70	0.012	7	0.457	0.233	0.183	0.050	1.823	151.96
2329	0.50	0.010	8	0.470	0.155	0.086	0.069	2.447	244.68
2330	0.20	0.008	9	0.458	0.144	0.093	0.051	1.856	231.99
2331	0.10	0.003	4	0.461	0.133	0.133	0.000	0.000	0.00
2332	0.20	0.009	5	0.462	0.288	0.280	0.008	0.289	32.07
2333	0.40	0.045	6	0.463	0.266	0.166	0.100	3.600	79.99
2334	0.40	0.057	7	0.457	0.211	0.183	0.028	1.021	17.91
2335	0.20	0.032	8	0.470	0.155	0.086	0.069	2.447	76.46
2336	0.40	0.057	9	0.458	0.488	0.093	0.395	14.374	252.18
2337	0.00	0.009	4	0.461	0.144	0.133	0.011	0.398	44.19
2338	0.00	0.037	5	0.462	0.433	0.280	0.153	5.519	149.18
2339	0.30	0.017	6	0.463	0.344	0.166	0.178	6.407	376.91
2340	0.00	0.017	7	0.457	0.188	0.183	0.005	0.182	10.73
2341	0.00	0.040	8	0.470	0.155	0.086	0.069	2.447	61.17
2342	0.00	0.082	9	0.458	0.344	0.093	0.251	9.134	111.39
2344	0.10	0.010	5	0.462	0.322	0.280	0.042	1.515	151.52
2346	0.30	0.009	7	0.457	0.200	0.183	0.017	0.620	68.89
2348	1.00	0.021	9	0.458	0.711	0.093	0.618	22.489	1070.91
2352	0.80	0.020	7	0.457	0.288	0.183	0.105	3.829	191.47
2353	0.10	0.029	8	0.470	0.144	0.086	0.058	2.057	70.92
2355	1.10	0.009	4	0.461	0.277	0.133	0.144	5.206	578.45
2357	0.50	0.079	6	0.463	0.444	0.166	0.278	10.007	126.67
2358	0.40	0.015	7	0.457	0.211	0.183	0.028	1.021	68.08
2359	0.10	0.009	8	0.470	0.122	0.086	0.036	1.277	141.84
2361	0.50	0.041	4	0.461	0.155	0.133	0.022	0.795	19.40
2363	0.70	0.092	6	0.463	0.944	0.166	0.778	28.006	304.41
2364	0.20	0.006	7	0.457	0.266	0.183	0.083	3.027	504.50
2365	0.50	0.044	8	0.470	0.133	0.086	0.047	1.667	37.88
2366	0.40	0.029	9	0.458	0.166	0.093	0.073	2.656	91.60
2367	3.30	0.442	4	0.461	0.844	0.133	0.711	25.705	58.16
2368	0.50	0.097	5	0.462	0.566	0.280	0.286	10.317	106.37
2370	0.30	0.018	7	0.457	0.277	0.183	0.094	3.428	190.45
2373	0.40	0.056	4	0.461	0.355	0.133	0.222	8.026	143.32
2374	0.30	0.029	5	0.462	0.533	0.280	0.253	9.127	314.72
2377	0.10	0.039	8	0.470	0.188	0.086	0.102	3.617	92.74
2379	0.10	0.002	4	0.461	0.200	0.133	0.067	2.422	1211.14

Cont.

Table 1 - cont.

S #	RD (ag)	SiO2 (ag)	Tri #	eff.	cpm (g)	B (cpm)	cpm(g)-B(cpm)	mBq	LLRD/SiO2 (mBq/ag)
2380	0.00	0.056	5	0.462	0.366	0.280	0.086	3.102	55.40
2381	0.10	0.025	6	0.463	0.322	0.166	0.156	5.616	224.62
2383	0.10	0.003	8	0.470	0.288	0.086	0.202	7.163	2387.71
2385	0.30	0.023	4	0.461	0.222	0.133	0.089	3.218	139.90
2386	0.60	0.079	5	0.462	0.511	0.280	0.231	8.333	105.49
2387	0.50	0.024	6	0.463	0.488	0.166	0.322	11.591	482.96
2388	0.30	0.026	7	0.457	0.344	0.183	0.161	5.872	225.83
2390	0.10	0.011	9	0.458	0.277	0.093	0.184	6.696	608.71
2391	0.00	0.013	4	0.461	0.311	0.133	0.178	6.435	495.02
2392	0.30	0.005	5	0.462	0.455	0.280	0.175	6.313	1262.63
2393	0.00	0.001	6	0.463	0.233	0.166	0.067	2.412	2411.81
2395	0.00	0.025	8	0.470	0.211	0.086	0.125	4.433	177.30
2396	0.20	0.055	9	0.458	0.277	0.093	0.184	6.696	121.74
2397	0.12	0.039	4	0.461	0.366	0.133	0.233	8.424	215.99
2398	0.11	0.031	5	0.462	0.477	0.280	0.197	7.107	229.25
2400	0.12	0.050	7	0.457	0.200	0.183	0.017	0.620	12.40
2402	0.13	0.031	9	0.458	0.477	0.093	0.384	13.974	450.77
2403	0.10	0.008	4	0.461	0.222	0.133	0.089	3.218	402.21
2404	0.12	0.006	5	0.462	0.411	0.280	0.131	4.726	787.64
2405	0.10	0.390	6	0.463	1.800	0.166	1.634	58.819	150.82
2407	0.12	0.002	8	0.470	0.088	0.086	0.002	0.071	35.46
2408	0.13	0.003	9	0.458	0.133	0.093	0.040	1.456	485.20
2409	0.13	0.008	4	0.461	0.211	0.133	0.078	2.820	352.49
2411	0.12	0.054	6	0.463	0.411	0.166	0.245	8.819	163.32
2412	0.14	0.028	7	0.457	0.222	0.183	0.039	1.422	50.80
2415	0.12	0.040	4	0.461	0.255	0.133	0.122	4.411	110.27
2417	0.10	0.018	6	0.463	0.266	0.166	0.100	3.600	199.98
2418	0.12	0.103	7	0.457	0.466	0.183	0.283	10.321	100.20
2421	0.12	0.006	9	0.458	0.233	0.093	0.140	5.095	849.10
2423	0.12	0.058	5	0.462	0.822	0.280	0.542	19.553	337.11
2424	0.12	0.130	6	0.463	2.177	0.166	2.011	72.390	556.85
2425	0.13	0.011	7	0.457	0.344	0.183	0.161	5.872	533.78
2426	0.12	0.025	6	0.463	0.444	0.166	0.278	10.007	400.29
2428	0.12	0.005	8	0.470	0.377	0.086	0.291	10.319	2063.83
2429	0.09	0.004	9	0.458	0.533	0.093	0.440	16.012	4002.91
2430	0.12	0.048	4	0.461	0.266	0.133	0.133	4.808	100.17
2432	0.12	0.004	6	0.463	0.277	0.166	0.111	3.996	998.92
2439	0.09	0.155	7	0.457	0.667	0.183	0.484	17.651	113.88
2448	0.12	0.007	4	0.461	0.255	0.133	0.122	4.411	630.10
2450	0.12	0.038	6	0.463	0.388	0.166	0.222	7.991	210.30
2451	0.08	0.001	7	0.457	0.311	0.183	0.128	4.668	4668.13
2453	0.00	0.025	9	0.458	0.188	0.093	0.095	3.457	138.28
2454	0.00	0.035	4	0.461	0.400	0.133	0.267	9.653	275.80
2455	0.00	0.032	5	0.462	0.366	0.280	0.086	3.102	96.95
2456	0.00	0.036	6	0.463	0.344	0.166	0.178	6.407	177.99
2461	0.00	0.037	5	0.462	0.411	0.280	0.131	4.726	127.73
2465	0.00	0.031	9	0.458	0.155	0.093	0.062	2.256	72.78
2466	0.00	0.029	4	0.461	0.177	0.133	0.044	1.591	54.85
2468	0.00	0.028	6	0.463	0.177	0.166	0.011	0.396	14.14
2472	0.00	0.007	4	0.461	0.233	0.133	0.100	3.615	516.48
2473	0.00	0.017	5	0.462	0.422	0.280	0.142	5.123	301.33
2482	0.00	0.003	8	0.470	0.300	0.086	0.214	7.589	2529.55
2485	0.00	0.091	5	0.462	0.933	0.280	0.653	23.557	258.87
2486	0.00	0.029	6	0.463	0.366	0.166	0.200	7.199	248.26
2487	0.00	0.046	7	0.457	0.233	0.183	0.050	1.823	39.64
2488	0.00	0.107	8	0.470	0.200	0.086	0.114	4.043	37.78

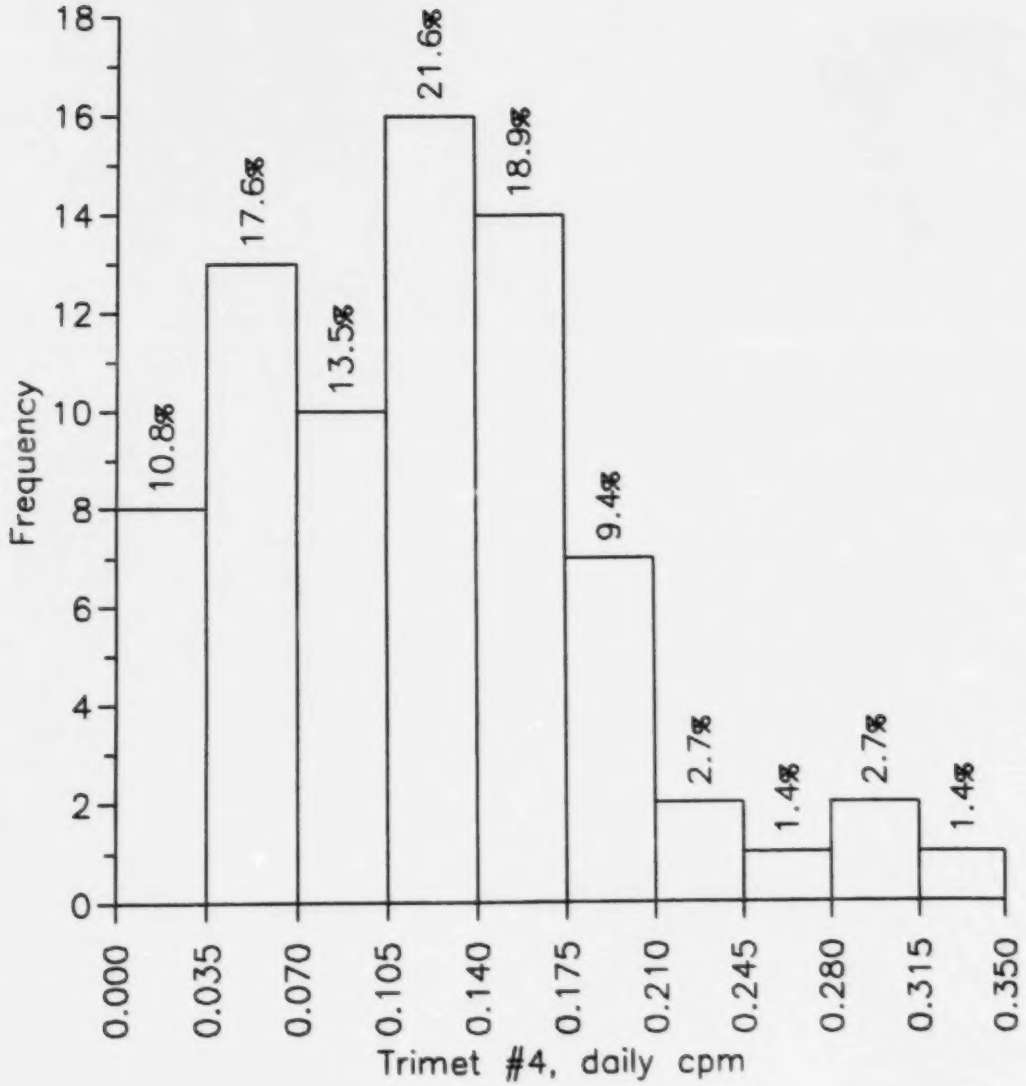

Fig. 1 - Scaler background (α-particle) count rate frequency histogram.

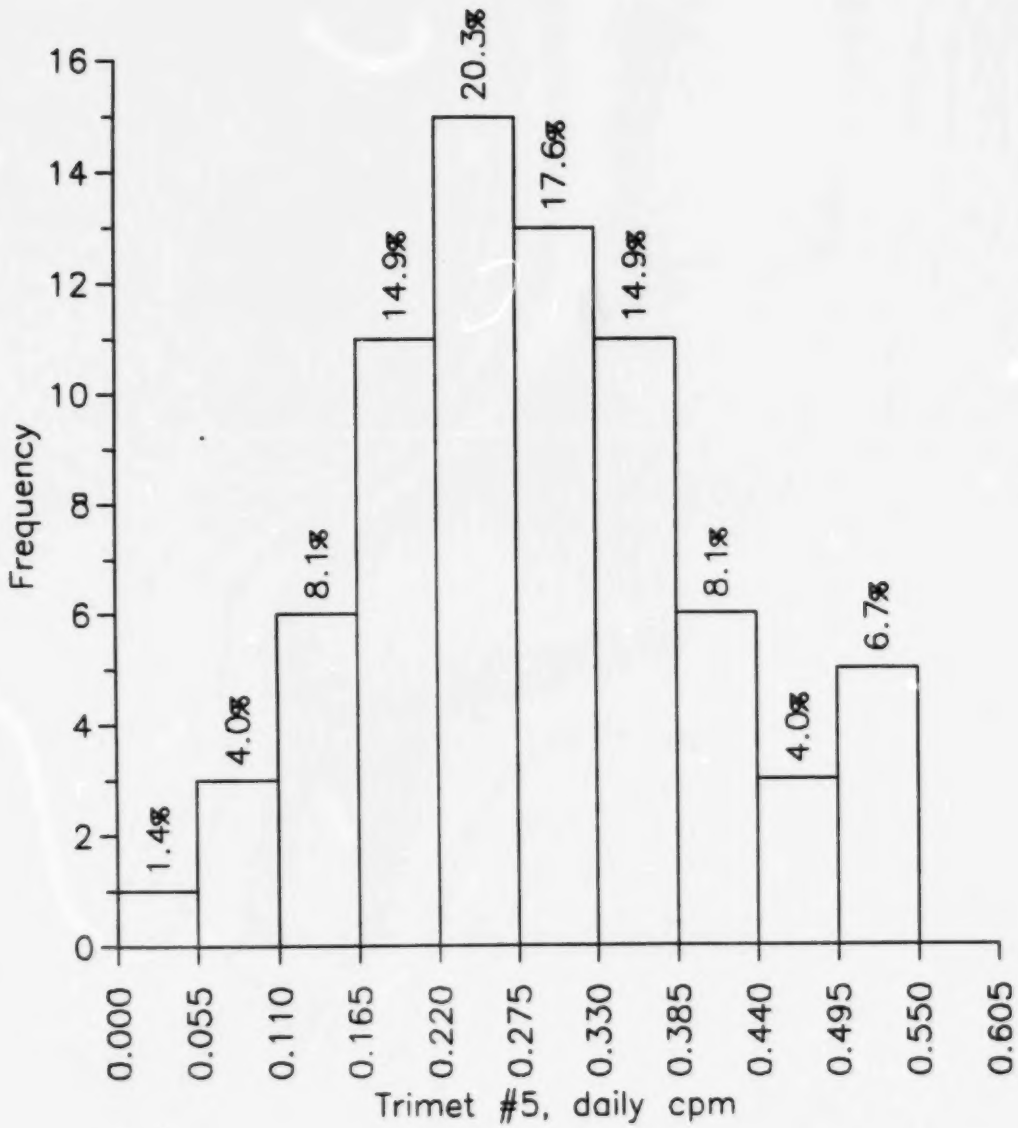

Fig. 2 - Scaler background (α-particle) count rate frequency histogram.

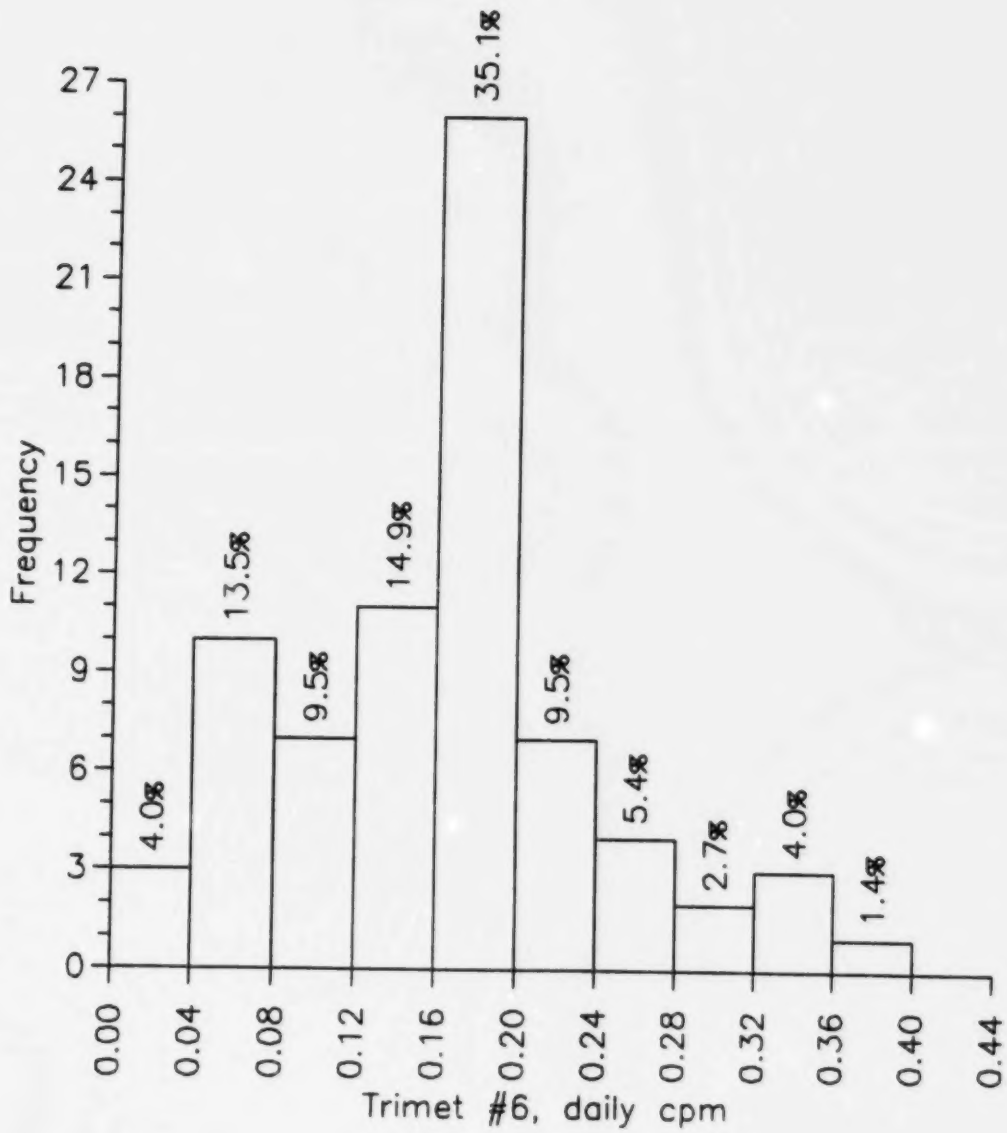

Fig. 3 - Scaler background (α-particle) count rate frequency histogram.

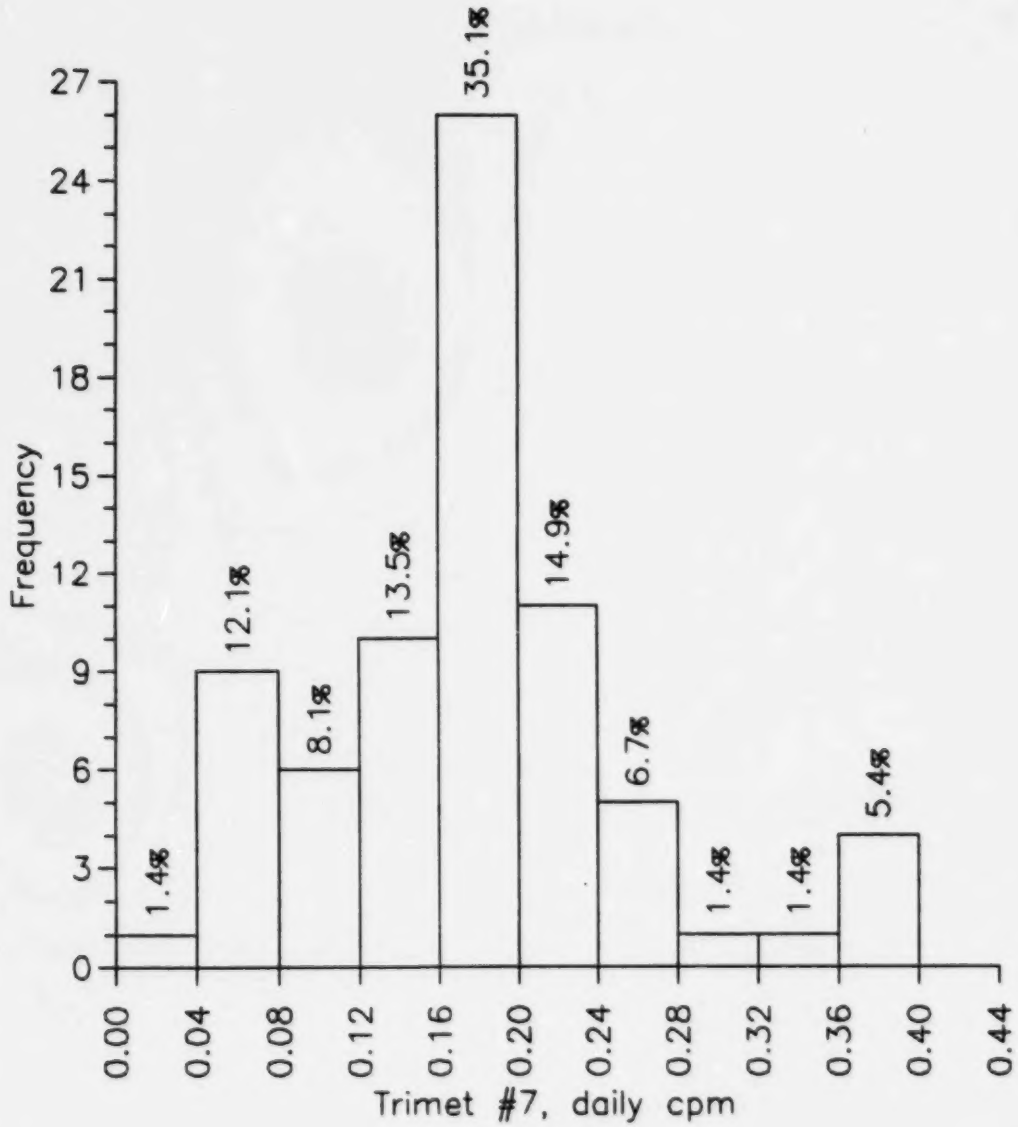

Fig. 4 - Scaler background (α-particle) count rate frequency histogram.

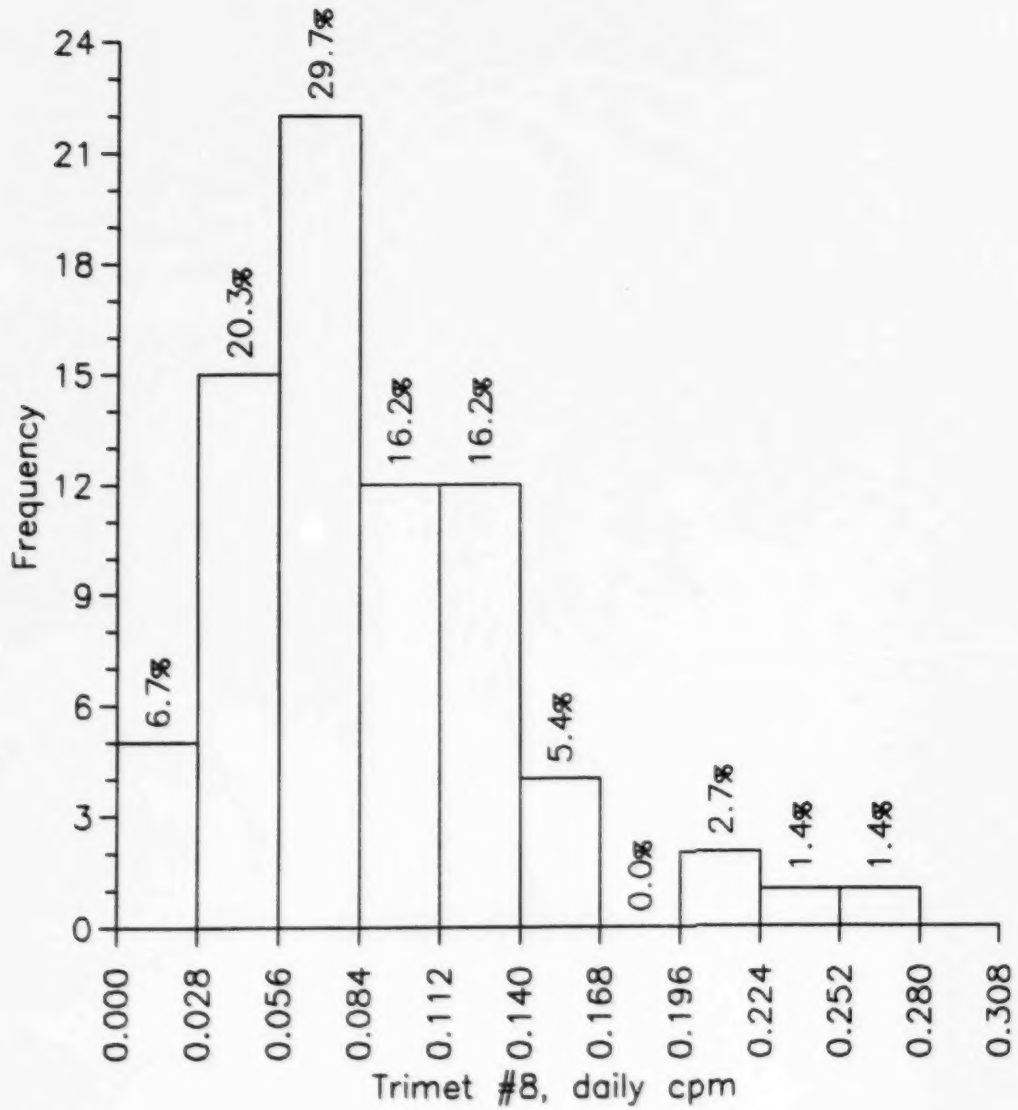

Fig. 5 - Scaler background (α-particle) count rate frequency histogram.

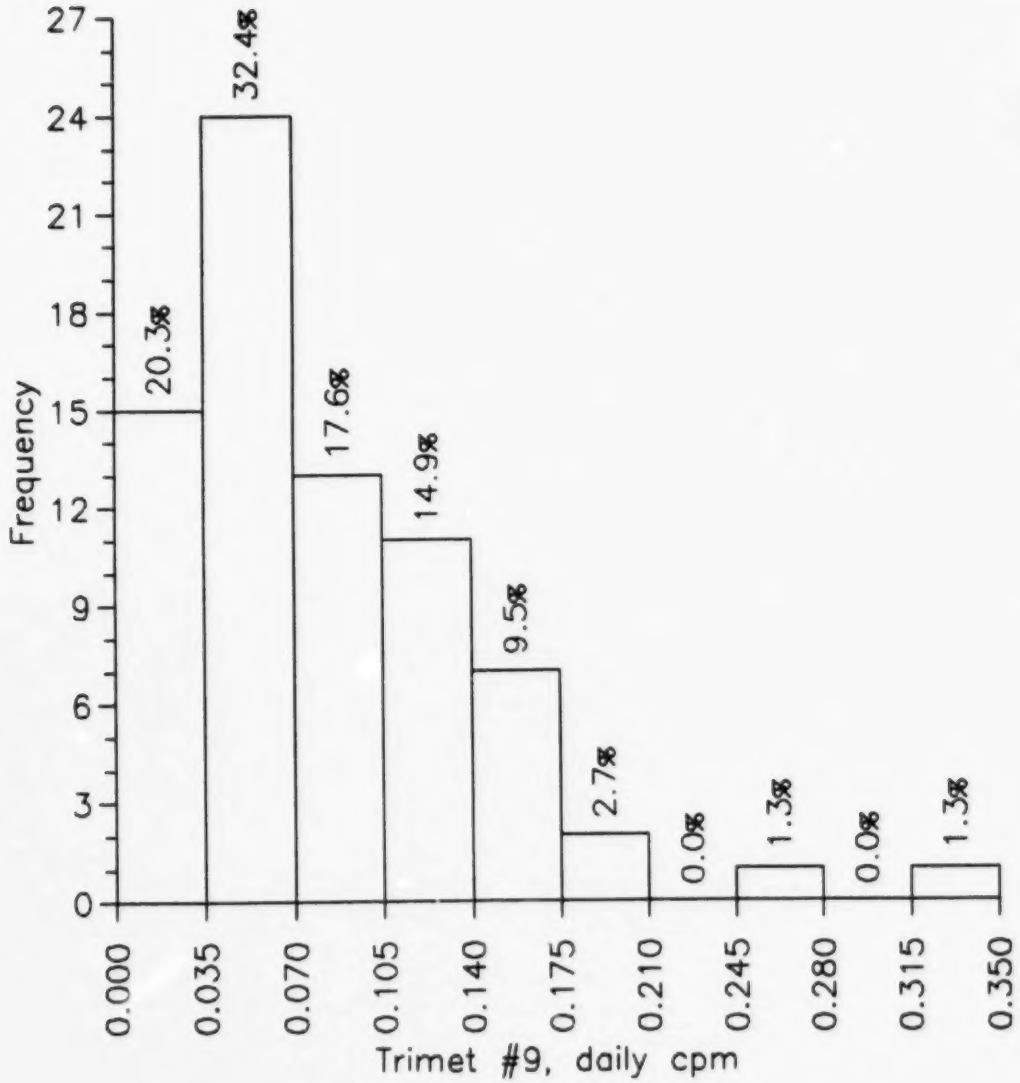

Fig. 6 - Scaler background (α-particle) count rate frequency histogram.

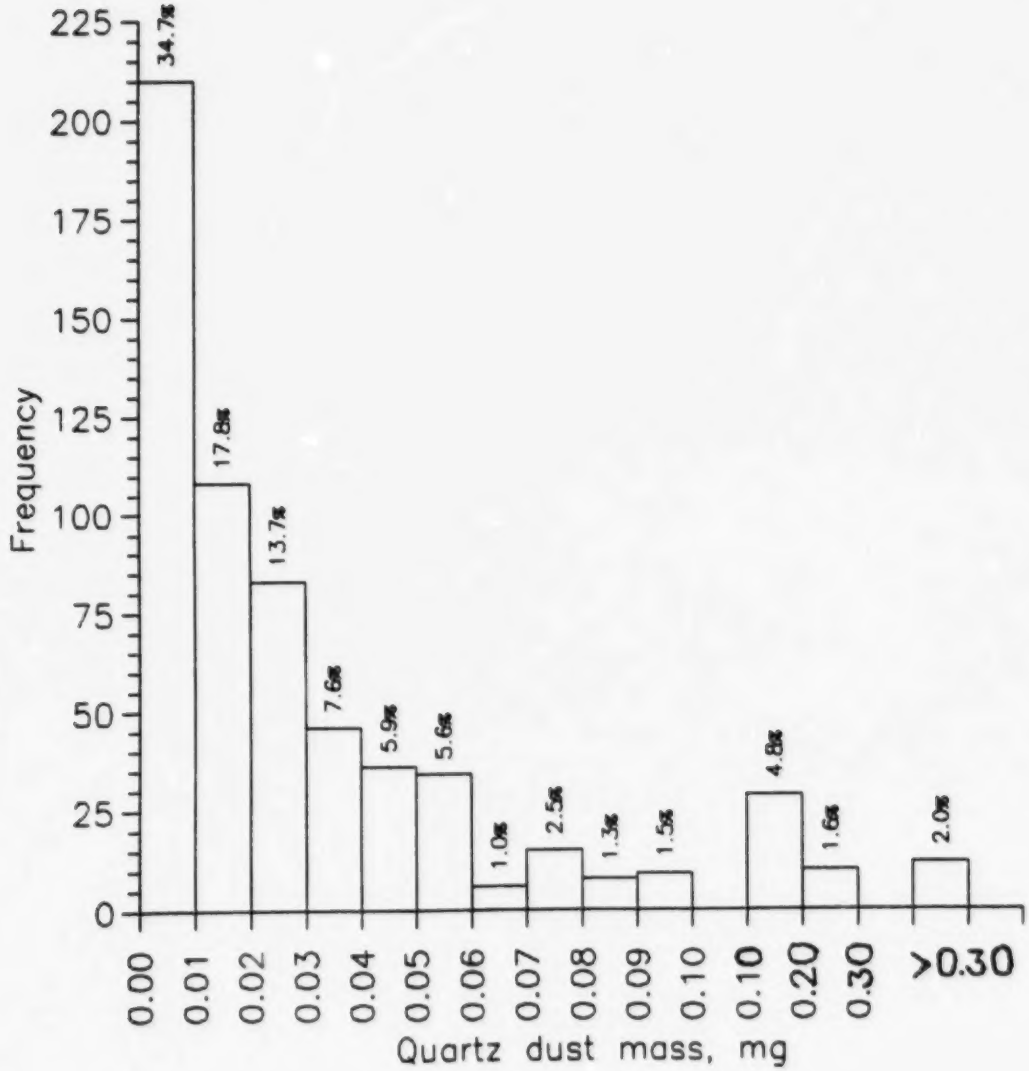

Fig. 7 - Quartz dust mass frequency histogram.

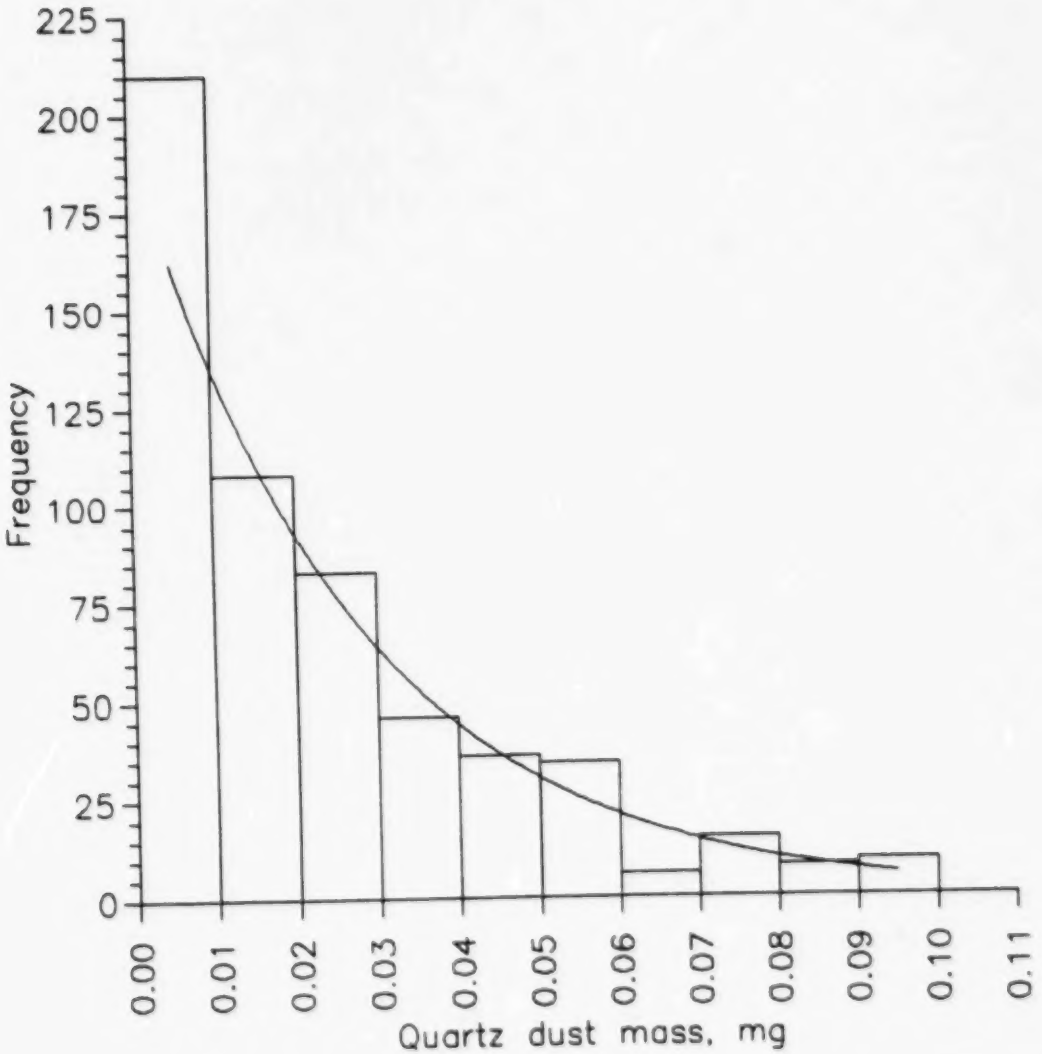

Fig. 8 - Quartz dust mass frequency histogram. Also shown is the best fitted curve by regression analysis.

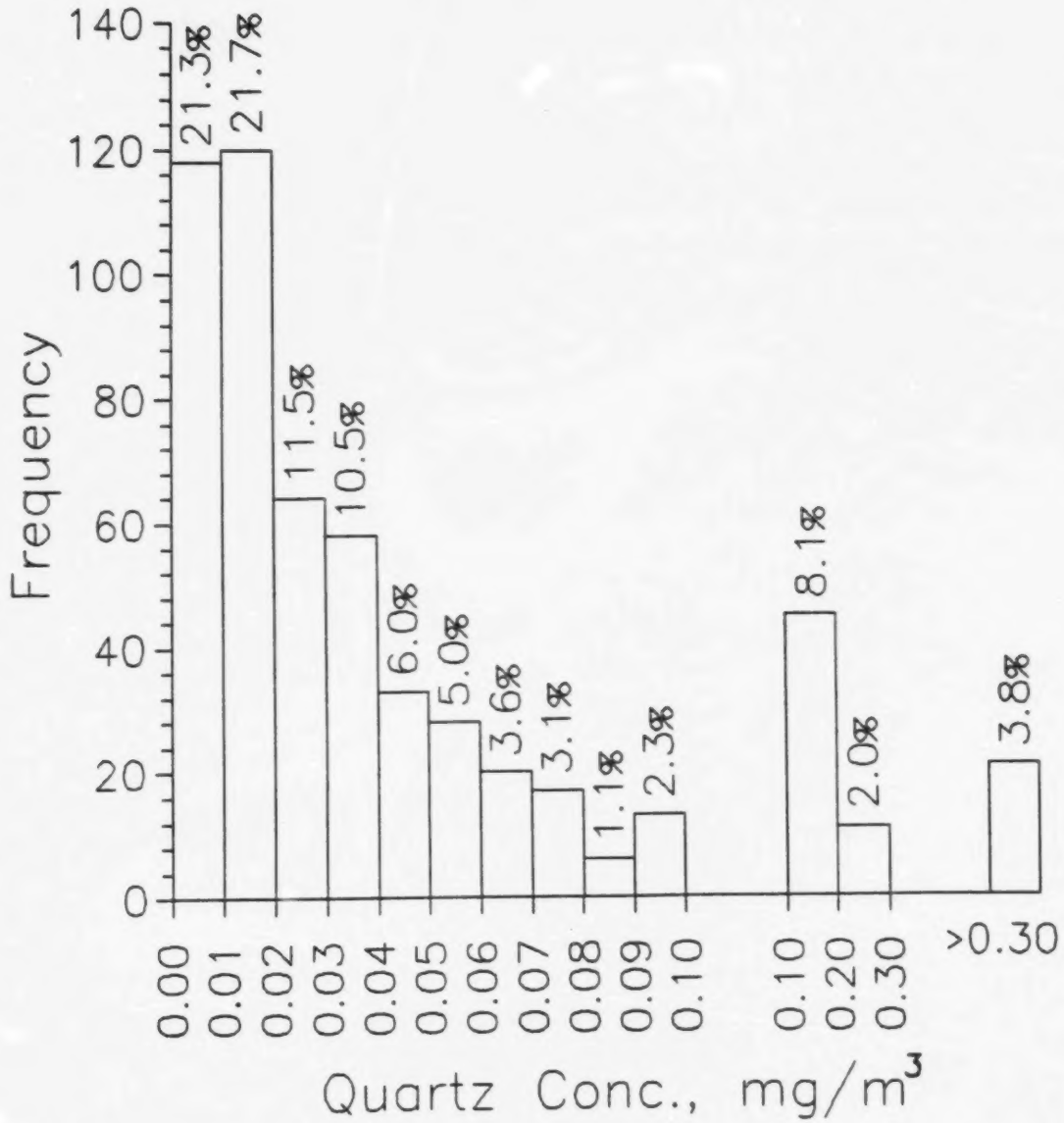

Fig. 9.- Silica (quartz) dust concentration frequency histogram.

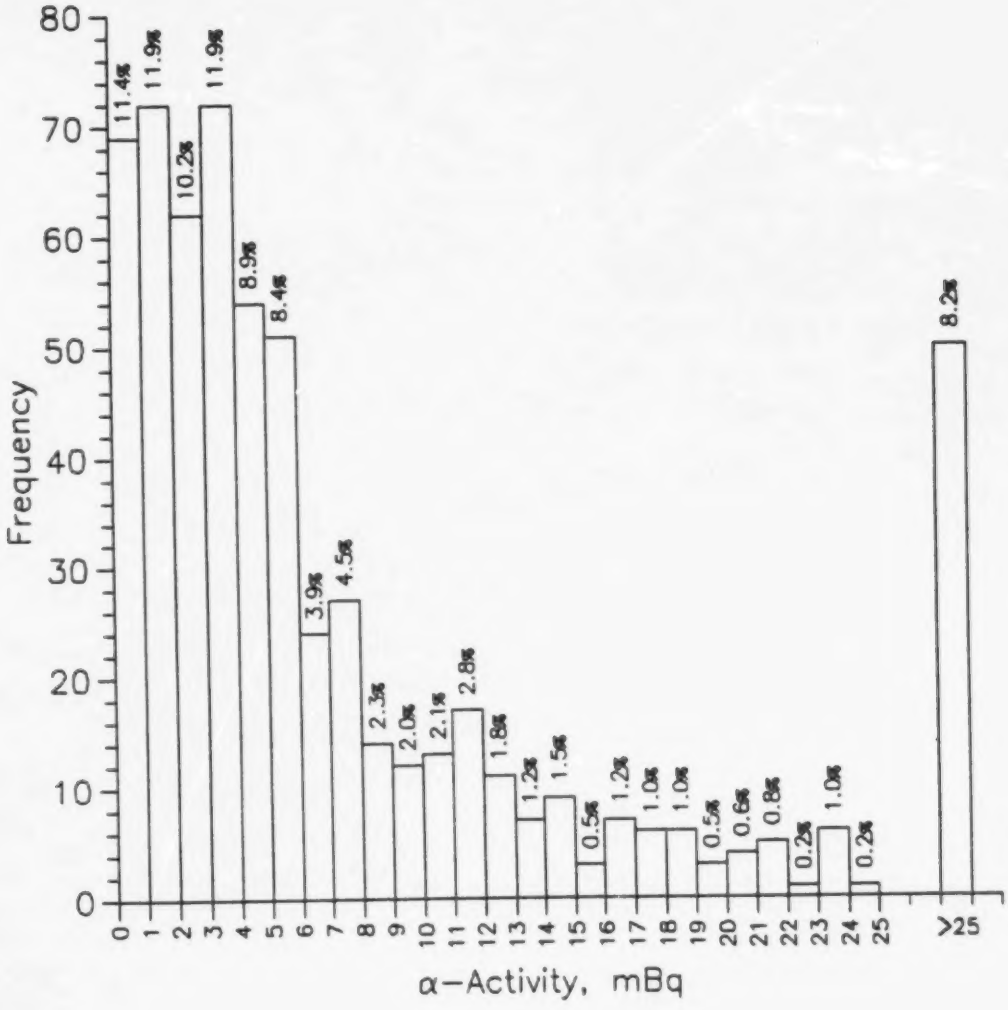

Fig. 10 - LLRD α-particle activity frequency histogram.

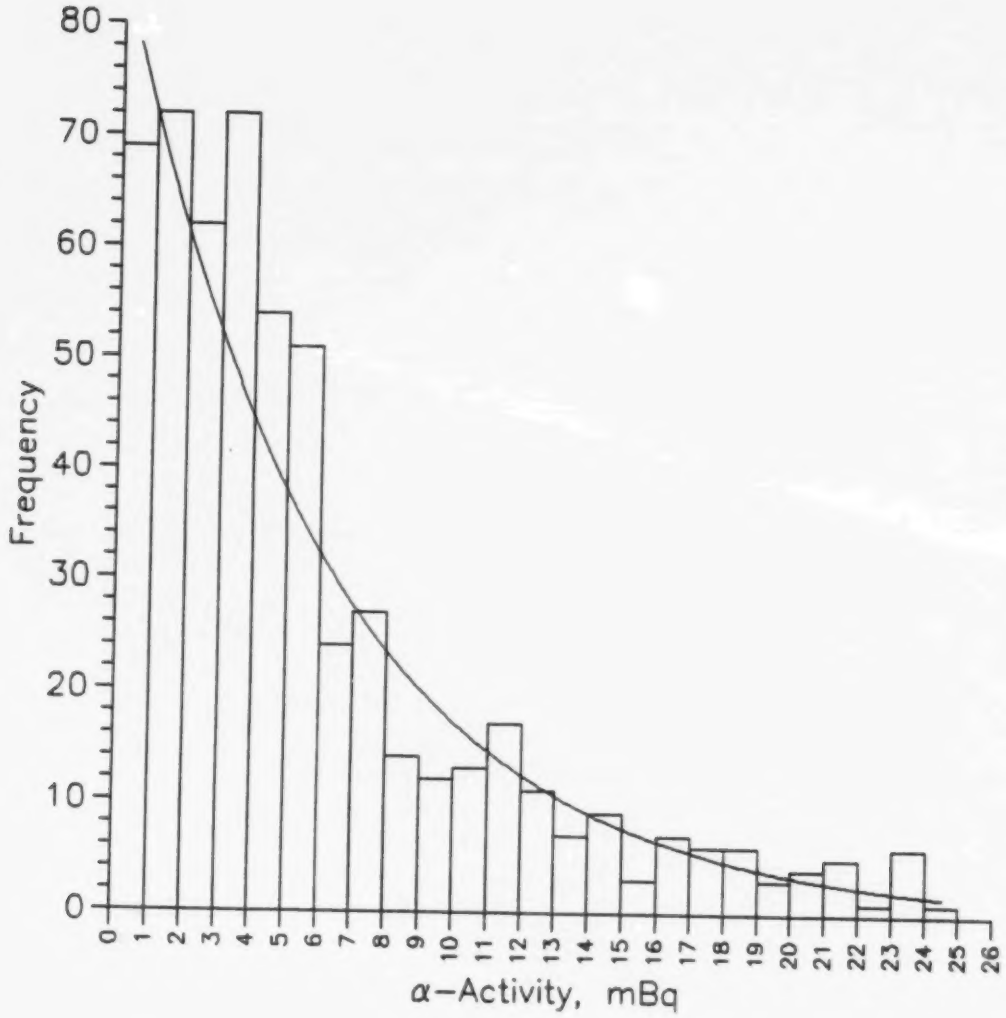

Fig. 11 - LLRD α-particle activity frequency histogram. Also shown is the best fitted curve by regression analysis.

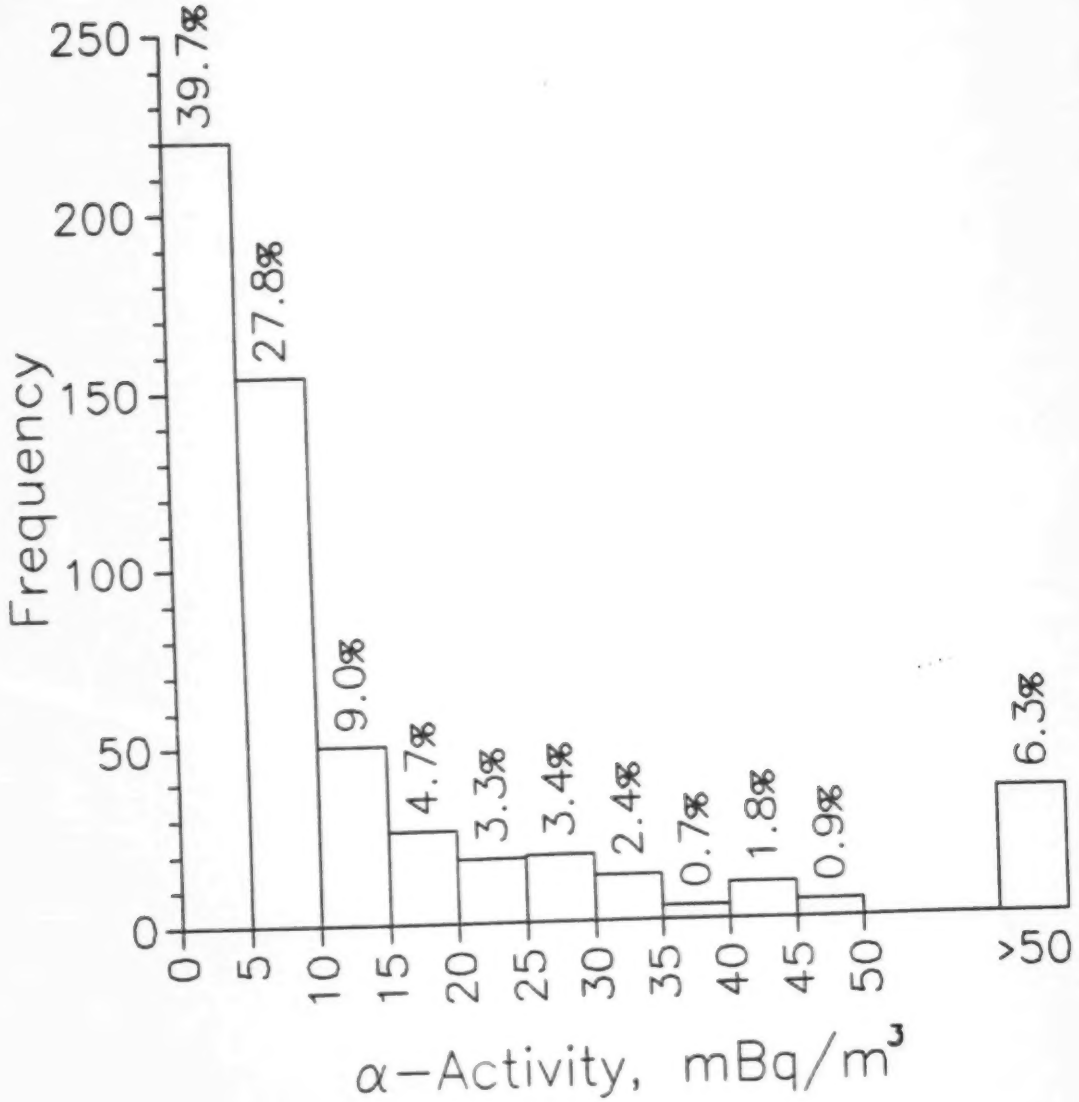

Fig. 12 - LLRD (α-particle) activity concentration frequency histogram.

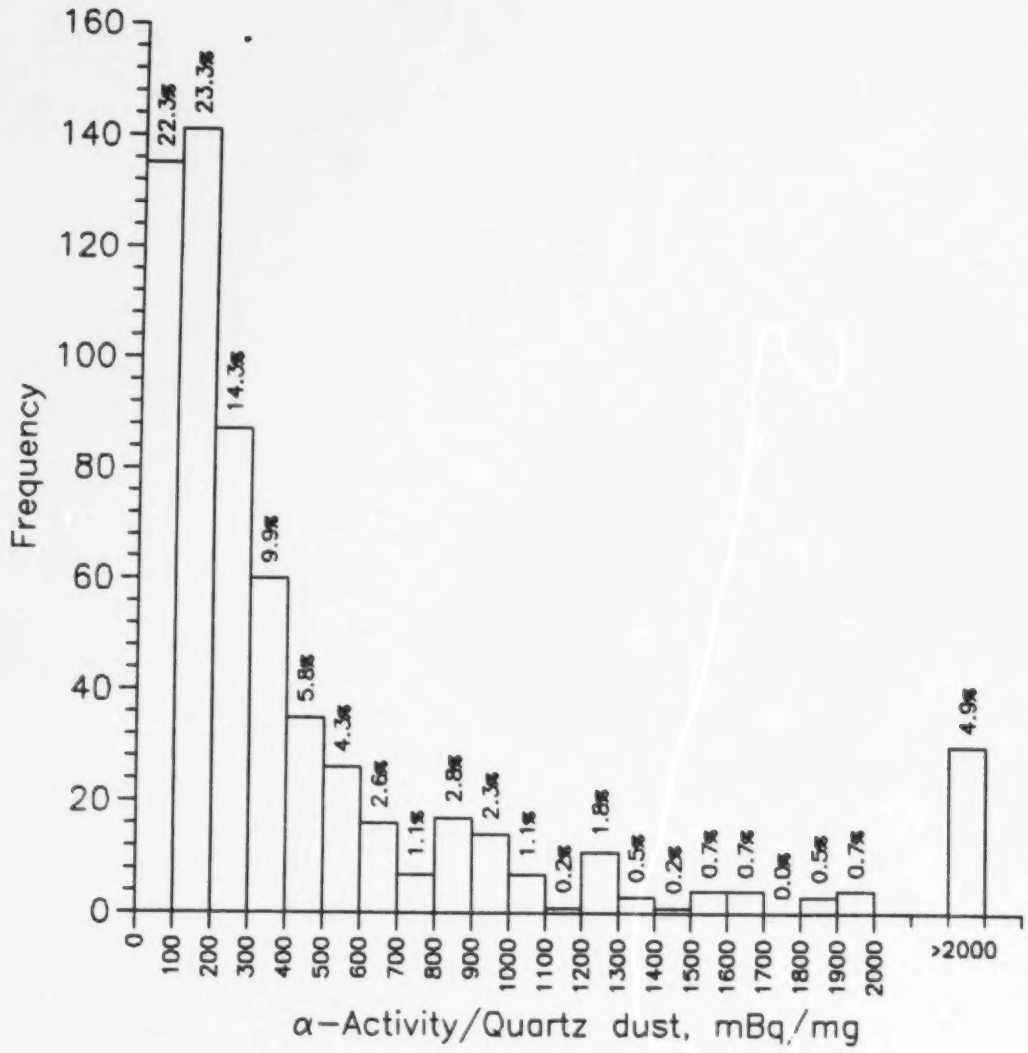

Fig. 13 - Specific activity (ratio of LLRD α-particle activity and quartz dust mass) frequency histogram.

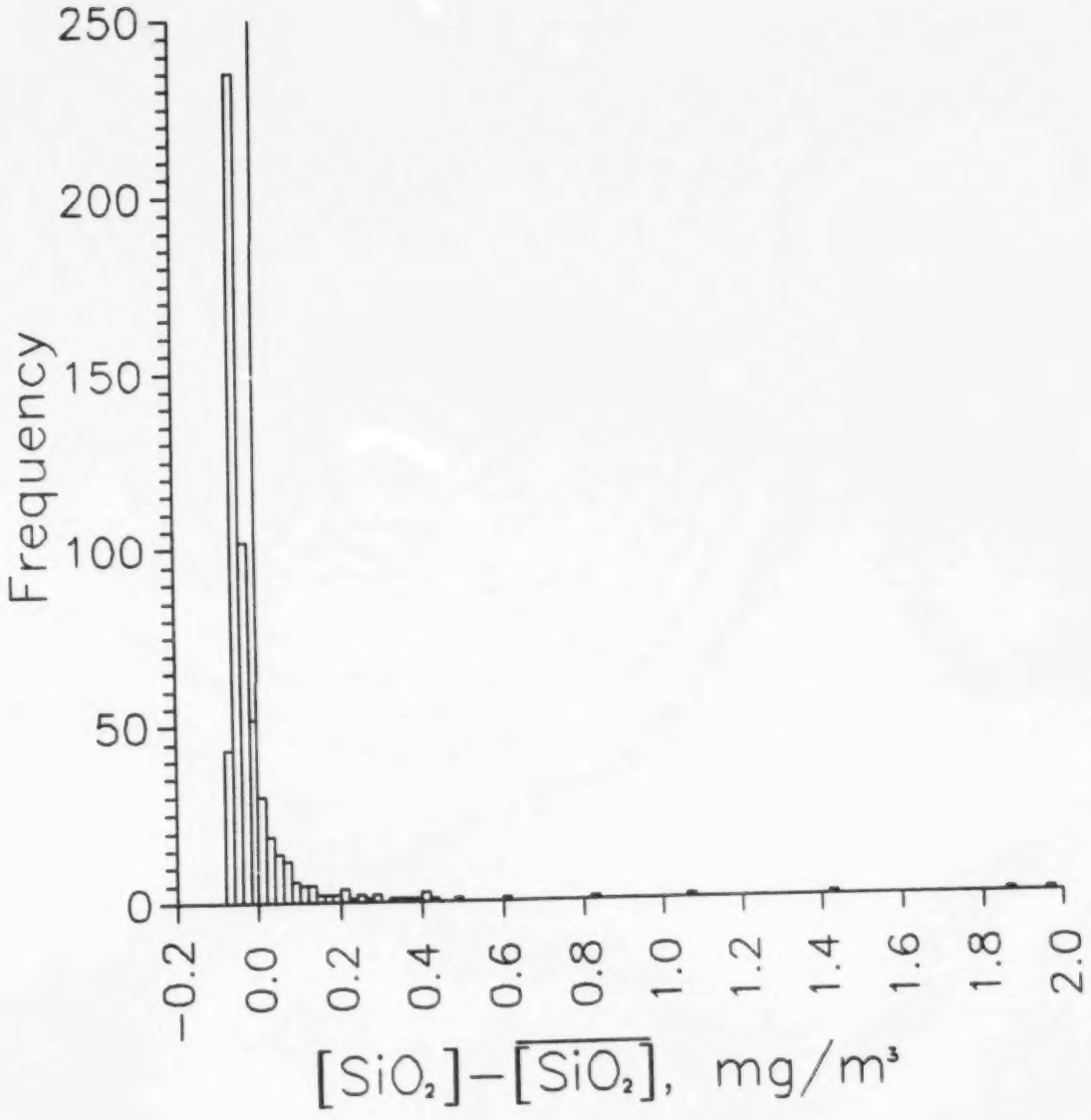

Fig. 14 - $[S_iO_2] - \overline{[S_iO_2]}$ frequency histogram.

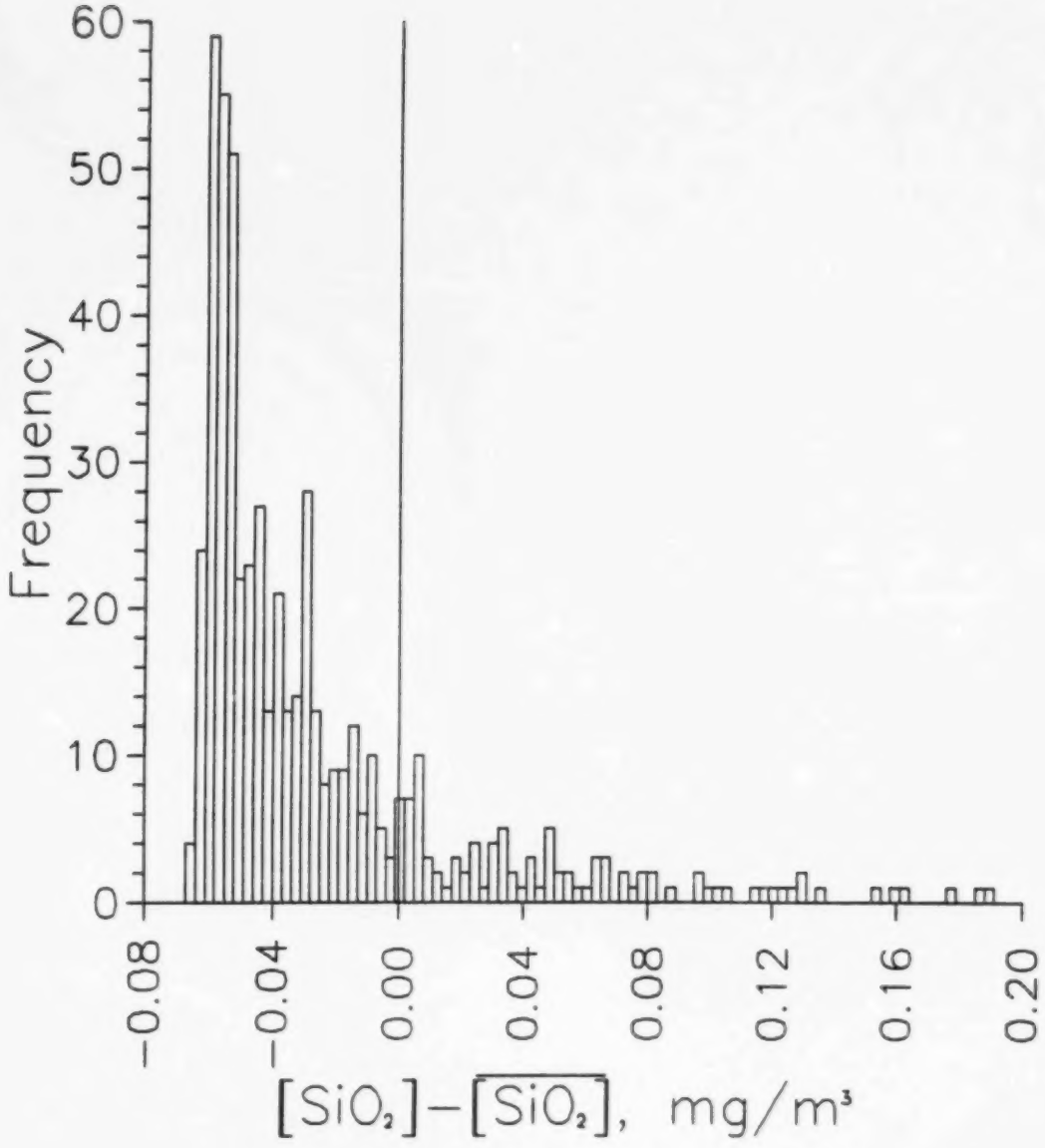

Fig. 15 - $[S_iO_2] - \overline{[S_iO_2]}$ frequency histogram.

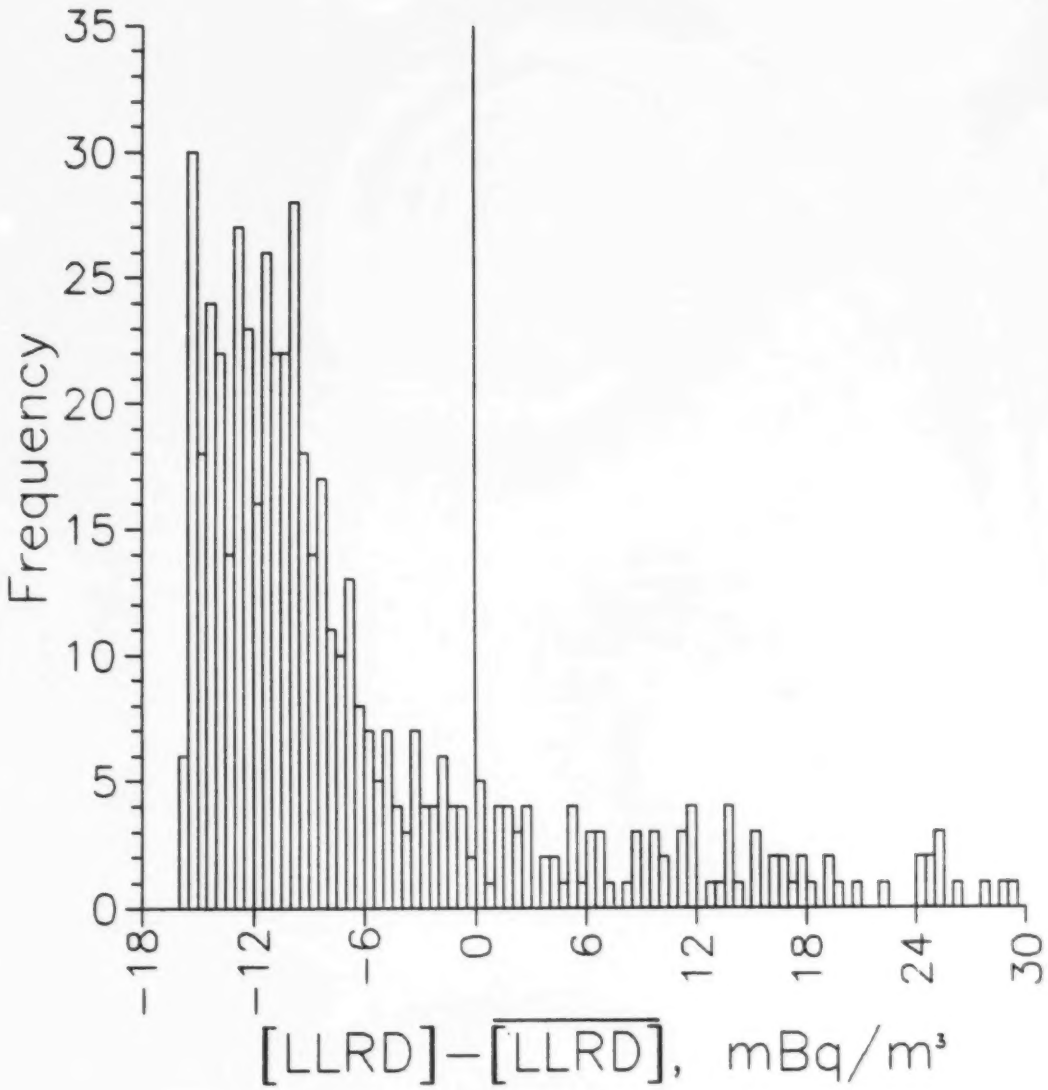

Fig. 16 - [LLRD] - $\overline{[LLRD]}$ frequency histogram.

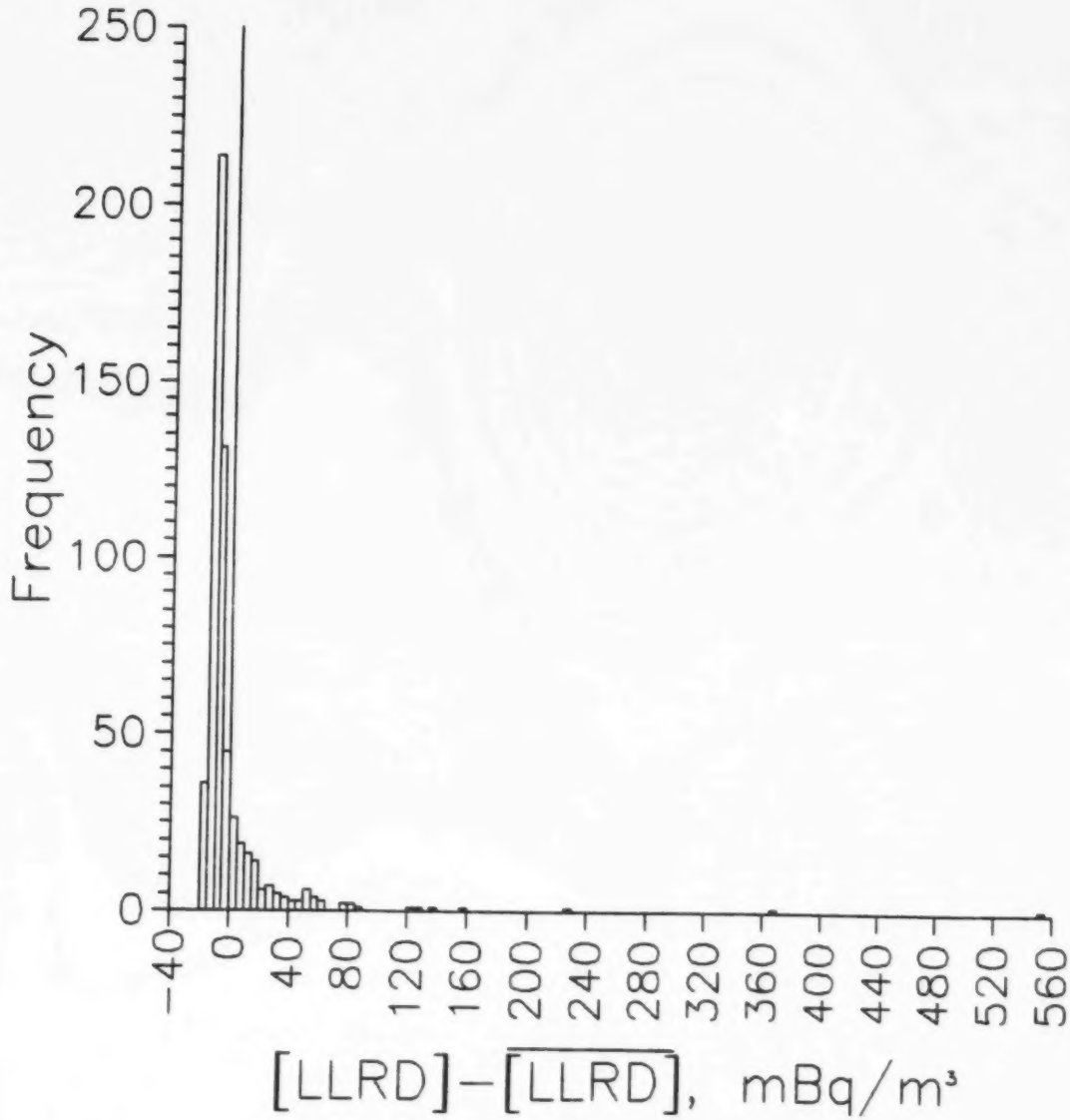

Fig. 17 - [LLRD] - $\overline{[LLRD]}$ frequency histogram.

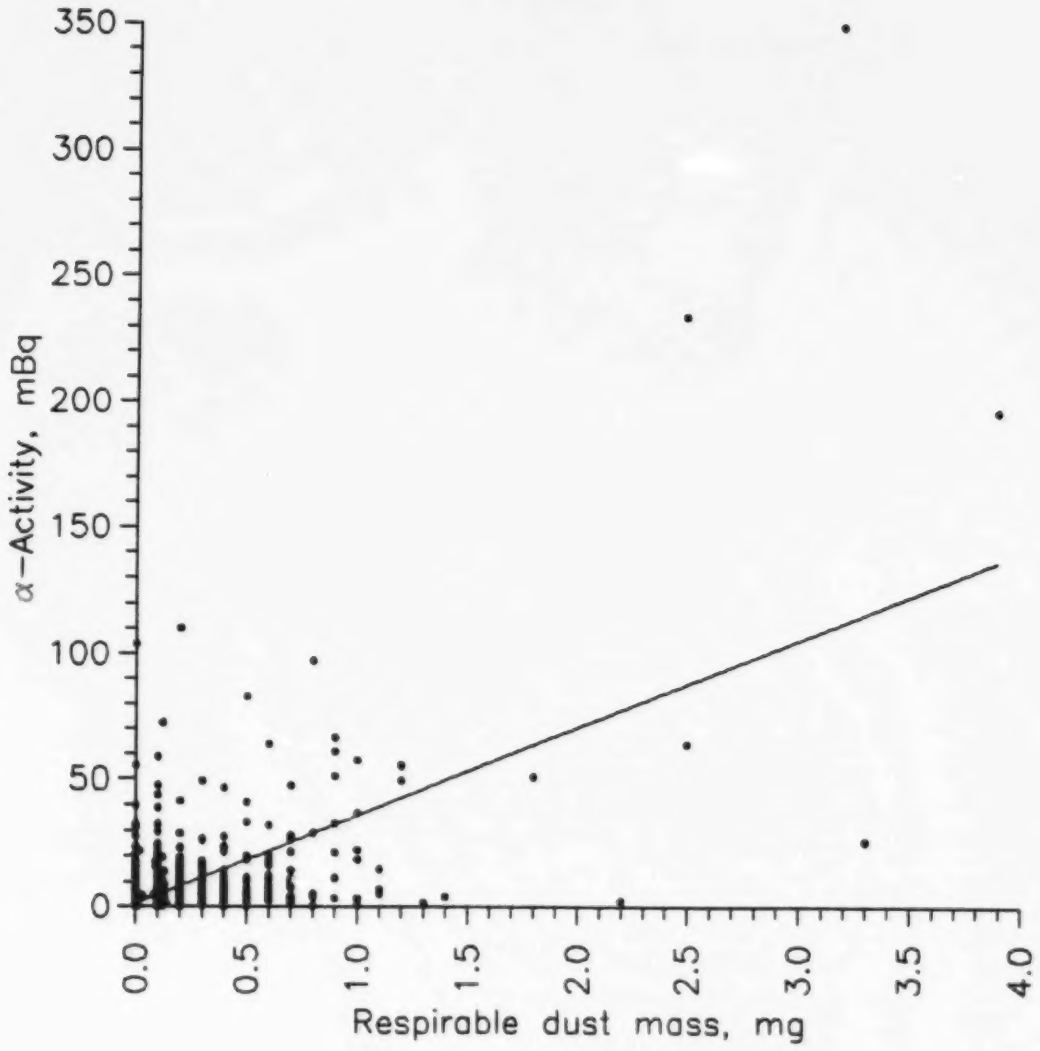

Fig. 18 - LLRD α-particle activity versus respirable dust mass. Also shown is the best fitted straight line through the data points by linear regression analysis.

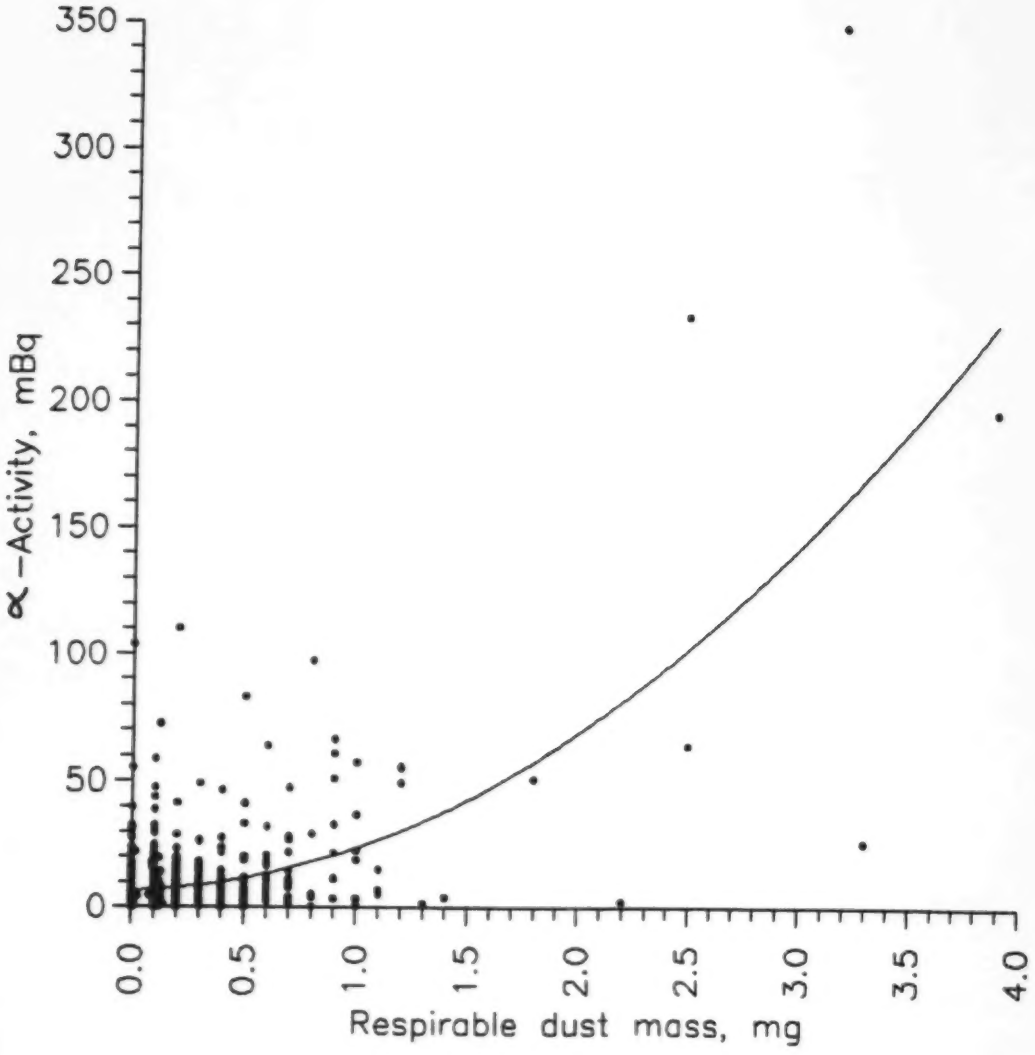

Fig. 19 - LLRD α-particle activity versus respirable dust mass. Also shown is the best fitted 2nd order polynomial through the data points by regression analysis.

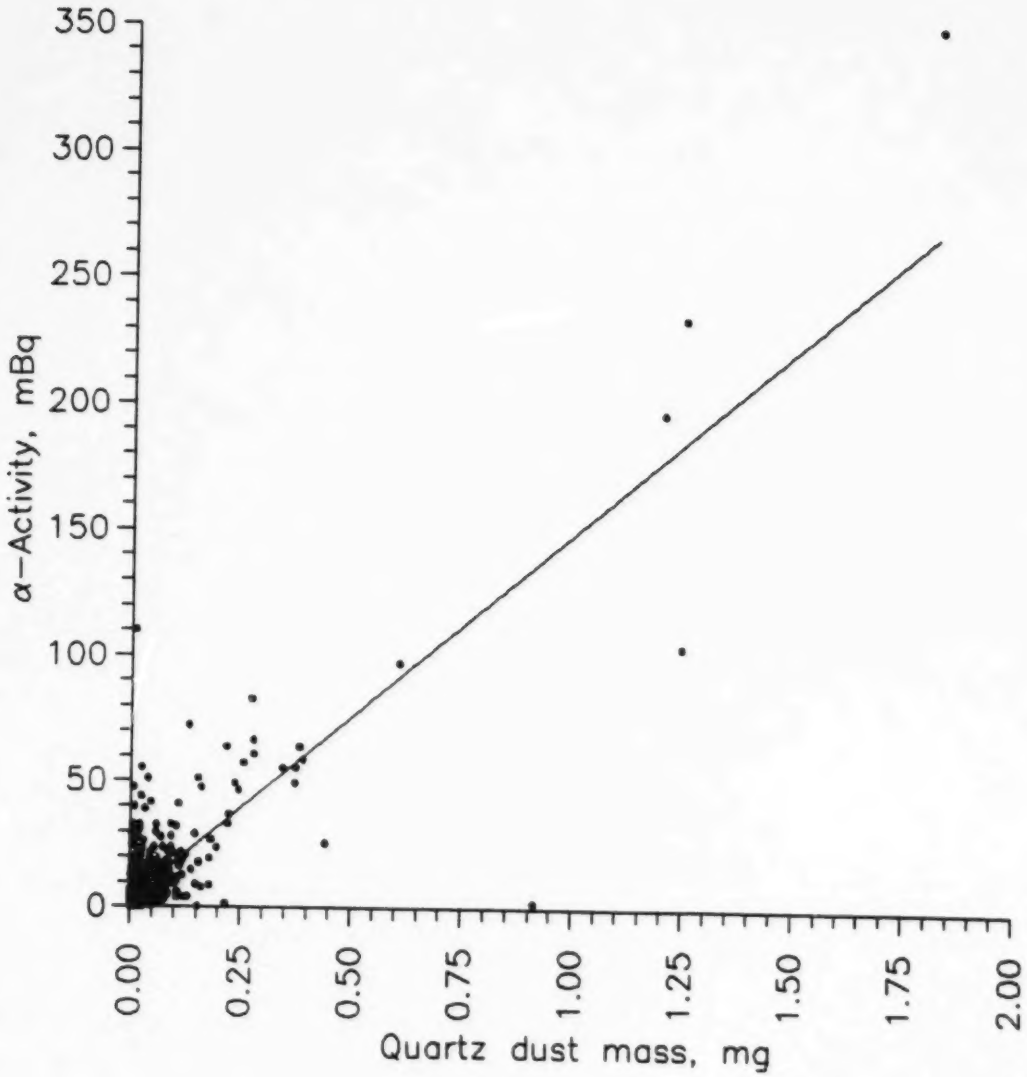

Fig. 20 - LLRD α-particle activity versus quartz dust mass. Also shown is the best fitted straight line to the data points by linear regression analysis.

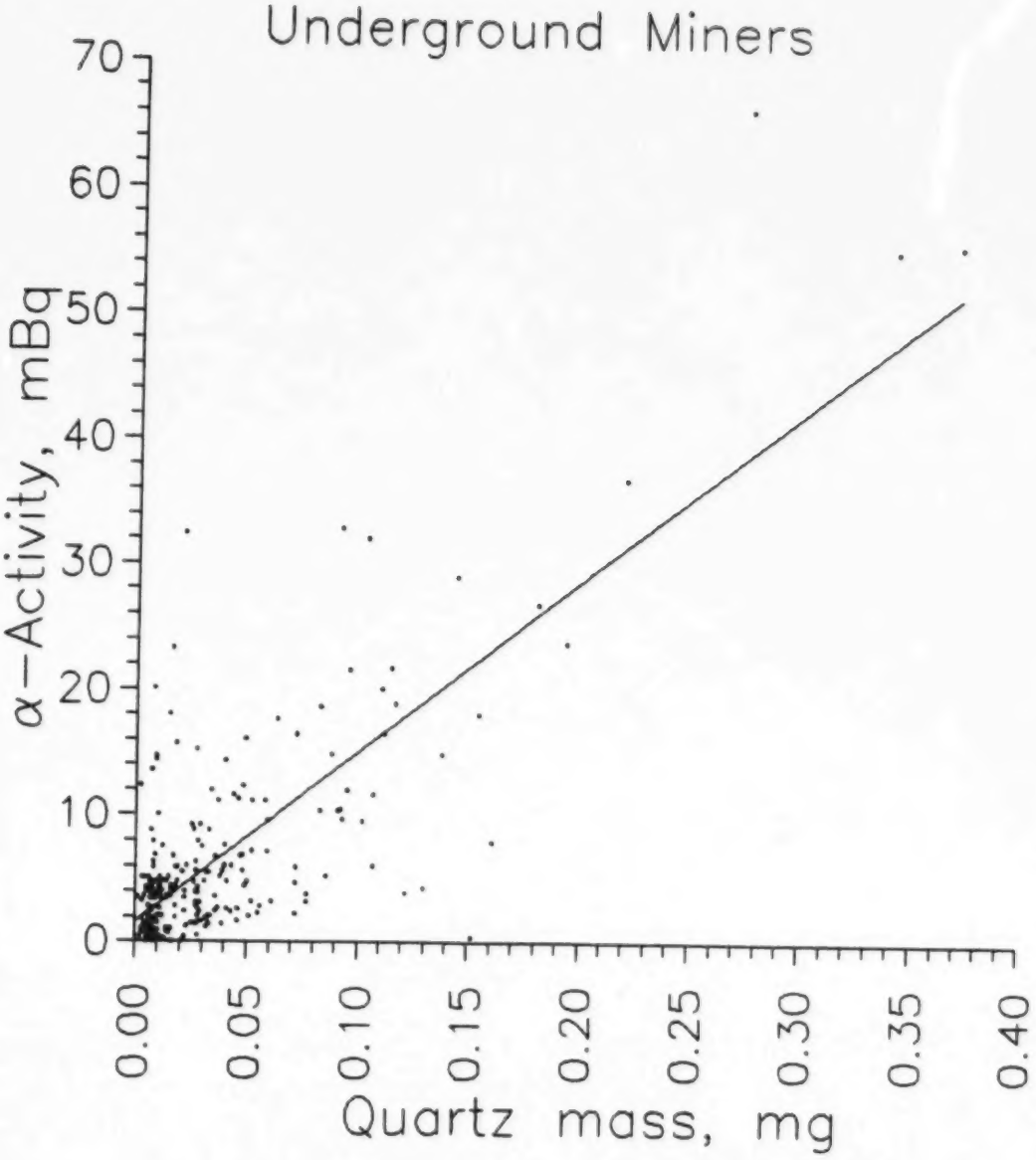

Fig. 21 - LLRD α-particle activity versus quartz dust mass for underground miners. Also shown is the best fitted straight line through the data points by linear regression analysis.

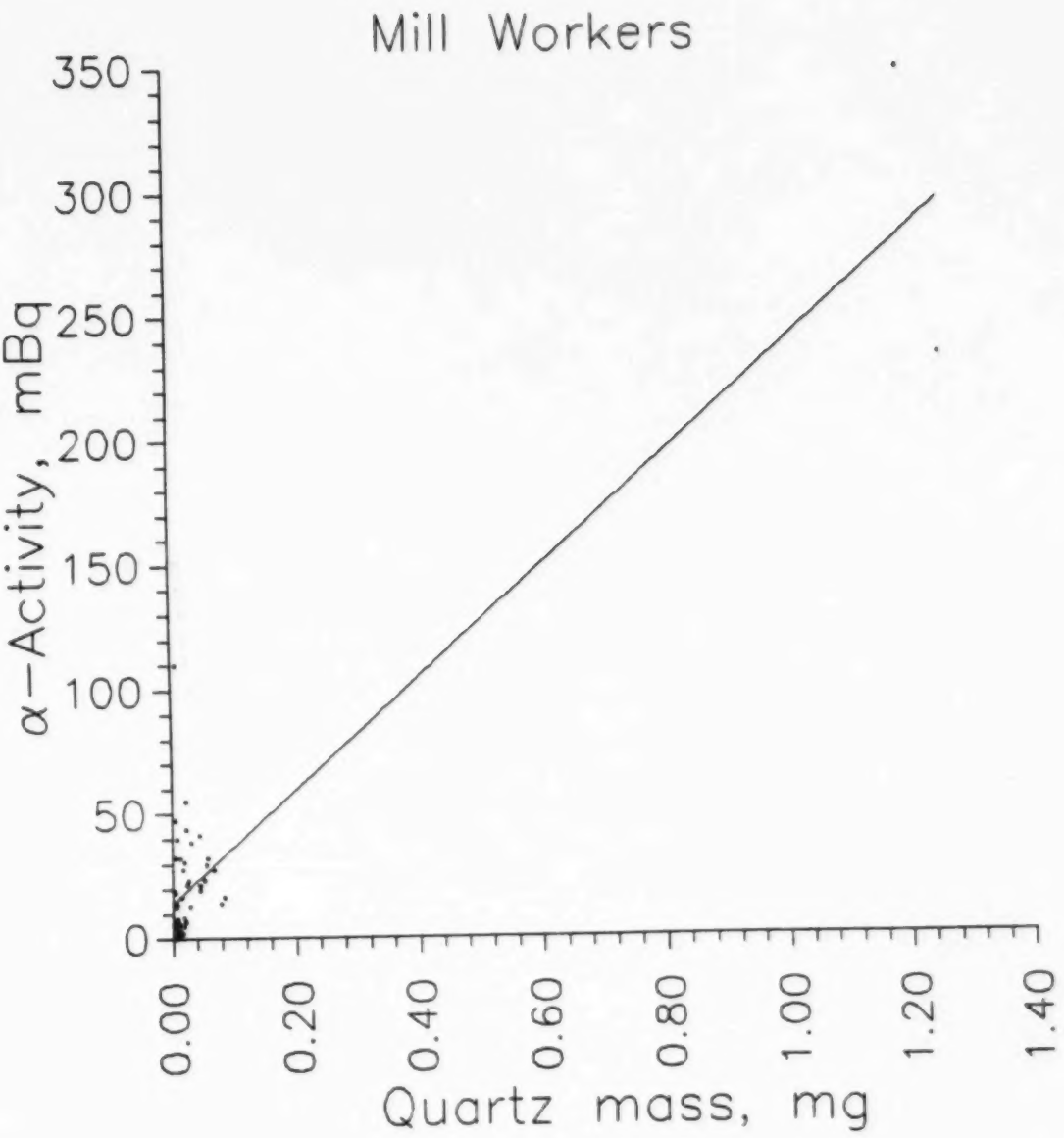

Fig. 22 - LLRD α-particle activity versus quartz dust mass for mill workers. Also shown is the best fitted straight line through the data points by linear regression analysis.

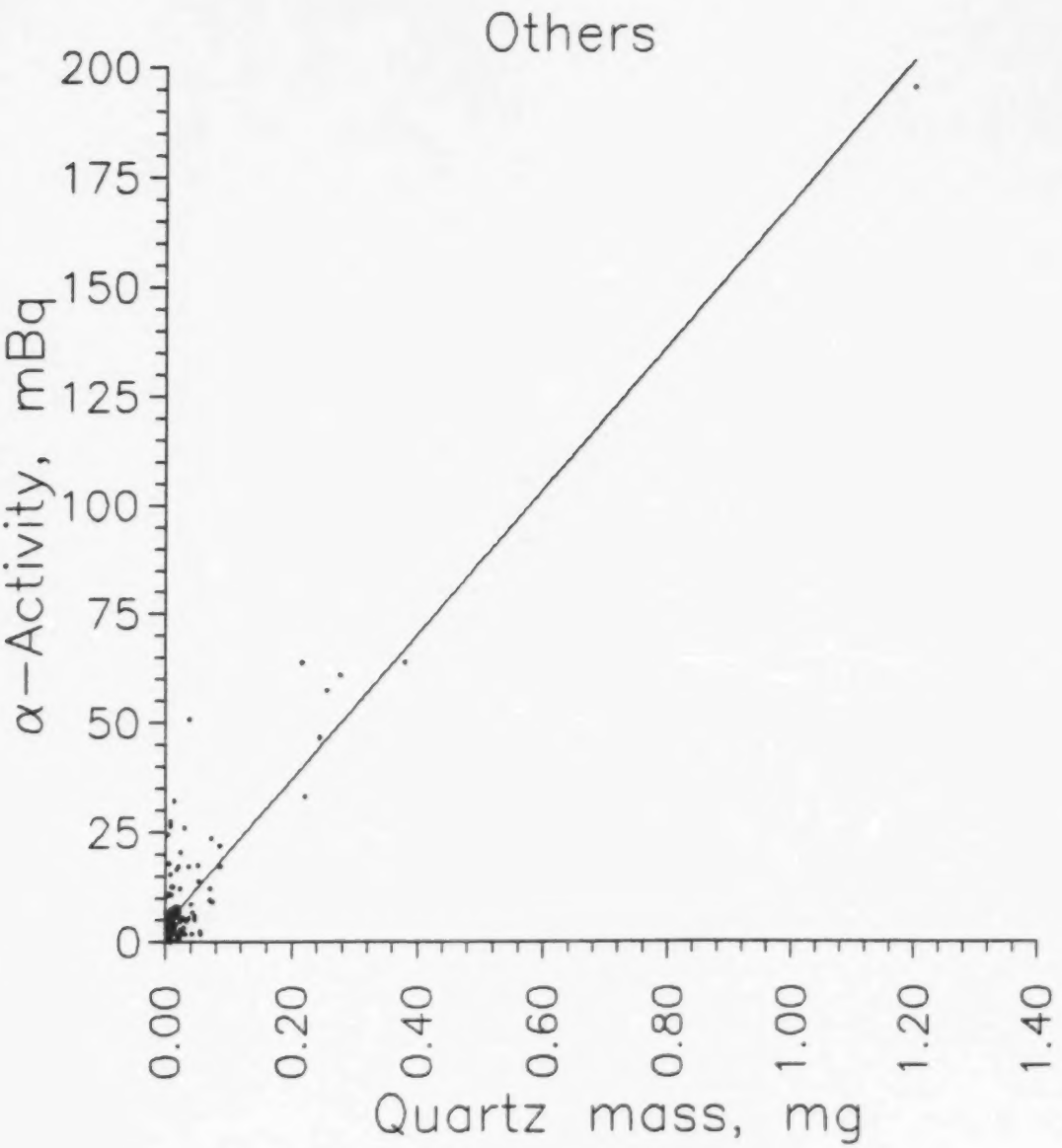

Fig. 23 - LLRD α-particle activity versus quartz dust mass for 'other' workers. Also shown is the best fitted straight line through the data points by linear regression analysis.